



저작자표시-비영리-변경금지 2.0 대한민국

이용자는 아래의 조건을 따르는 경우에 한하여 자유롭게

- 이 저작물을 복제, 배포, 전송, 전시, 공연 및 방송할 수 있습니다.

다음과 같은 조건을 따라야 합니다:



저작자표시. 귀하는 원저작자를 표시하여야 합니다.



비영리. 귀하는 이 저작물을 영리 목적으로 이용할 수 없습니다.



변경금지. 귀하는 이 저작물을 개작, 변형 또는 가공할 수 없습니다.

- 귀하는, 이 저작물의 재이용이나 배포의 경우, 이 저작물에 적용된 이용허락조건을 명확하게 나타내어야 합니다.
- 저작권자로부터 별도의 허가를 받으면 이러한 조건들은 적용되지 않습니다.

저작권법에 따른 이용자의 권리는 위의 내용에 의하여 영향을 받지 않습니다.

이것은 [이용허락규약\(Legal Code\)](#)을 이해하기 쉽게 요약한 것입니다.

[Disclaimer](#)

공학석사 학위논문

IGBT 모듈 냉각을 위한 루프 히트파이프 시스템의 성능 분석

Performance analysis of a loop heat pipe system for
IGBT module application

2022 년 8 월

서울대학교 대학원

기계항공공학부

김 명 수

IGBT 모듈 냉각을 위한 루프히트파이프 시스템의 성능 분석

Performance analysis of a loop heat pipe system for
IGBT module application

지도교수 김 민 수

이 논문을 공학석사 학위논문으로 제출함

2022 년 4 월

서울대학교 대학원

기계항공공학부

김 명 수

김 명 수의 공학석사 학위논문을 인준함

2022 년 6 월

위 원 장 : 송 한 호 (인)

부위원장 : 김 민 수 (인)

위 원 : 박 상 욱 (인)

Abstract

Performance analysis of a loop heat pipe system for IGBT module application

Myoung Soo Kim

Mechanical and Aerospace Engineering

The Graduate School

Seoul National University

Recently, the importance of the railroad industry is increasing as a low-carbon, high-efficiency, mass transportation method. In particular, the decentralized-power type train is preferred because of its excellent acceleration and transport efficiency compared to the centralized-power type train, and related technology developments

are actively taking place. In the case of decentralized–power type high–speed railway, a propulsion system is installed for each vehicle, so there is a limited space for a cooling system. Accordingly, the importance of cooling performance and efficient space utilization of the cooling system is increasing.

In this study, a loop type heat pipe was studied for temperature management of IGBT which is a semiconductor transistor applied to high–speed railway and subway propulsion systems. It was applied to increase the amount of cooling capacity per unit volume and the uniformity of the heat.

To analyze the applicability, three heat pipes were designed and manufactured. The performance of each heat pipe was compared by experiments. Theoretical analysis was conducted in order to manufacture the loop type heat pipe. Experiments were conducted regarding the optimal operating conditions to measure the accurate performance. An experiment was performed to confirm the sort of refrigerant and its charging rate, and it could be experimentally verified that the optimal condition was when the water was selected as the refrigerant with charging rate of 34.4%.

The conventional and loop type heat pipe experiments were conducted by simulating the high-speed railway or subway operating environment. The performance of each manufactured heat pipe was compared and analyzed while increasing the heat load of the simulated IGBT from 1800 W to 2400 W in a forced convection environment. As a result, the maximum temperature of the IGBT was lower when the loop type heat pipe was used, and the maximum cooling capacity was also calculated to be larger. Both heat pipes were satisfied the target performance for IGBT cooling.

Considering the operating life of the IGBT, the temperature uniformity of the IGBT is also an important cooling performance. An experiment was conducted to compare the temperature uniformity of the IGBT cooled by the heat pipe, and more improved results were obtained by the loop type.

It has been experimentally proven that the loop type heat pipe can increase the cooling efficiency for the decentralized-power system. At the same time, it was confirmed that a loop type heat pipe could be an efficient cooling method when considering the high density and miniaturization of future semiconductor components.

Keyword: Loop heat pipe, IGBT module, Cooling capacity,
Temperature uniformity, Decentralized-power type train

Student Number: 2017-26361

Table of Contents

| | |
|--|-------|
| Abstract | i |
| Contents | v |
| List of Tables..... | viii |
| List of Figures | ix |
| Nomenclatures | xiii |
| Subscript | xvi |
| Chapter 1. Introduction..... | 1 |
| 1.1 Background of the study | 1 |
| 1.2 Literature review | 9 |
| 1.2.1 Cooling of electric devices method..... | 9 |
| 1.2.2 Loop heat pipe as a cooling system | 10 |
| 1.3 Purpose and scope..... | 12 |
| Chapter 2. Design and manufacture | 15 |
| 2.1 Concept Design | 15 |
| 2.2 Element design..... | 19 |

| | |
|---|----|
| 2.2.1 Target specification..... | 19 |
| 2.2.2 Refrigerant and pipe | 23 |
| 2.2.2.1 Refrigerant..... | 23 |
| 2.2.2.2 Specification of pipe | 26 |
| 2.2.2.3 Wick structure | 27 |
| 2.2.3 Operation limits..... | 28 |
| 2.2.2.1 Capillary limit | 28 |
| 2.2.2.2 Boiling limit..... | 31 |
| 2.2.2.3 Sonic limit | 31 |
| 2.2.2.4 Entrainment limit | 32 |
| 2.3 Manufacture of heat pipe | 34 |
| Chapter 3. Experimental setup and facility..... | 43 |
| 3.1 Simulation of environment..... | 43 |
| 3.1.1 Simulation of IGBT module..... | 43 |
| 3.1.2 Operating environment simulation..... | 49 |
| 3.2 Experimental setup..... | 52 |
| 3.2.1 Setup of heat pipe | 52 |

| | |
|---|-----|
| 3.2.2 Experiment facility | 53 |
| 3.2.3 Experiment case | 63 |
| Chapter 4. Experimental results | 68 |
| 4.1 Optimal working conditions..... | 68 |
| 4.1.1 Determining refrigerant..... | 68 |
| 4.1.2 Optimal filling rate of refrigerant | 70 |
| 4.2 Results of performance | 78 |
| 4.2.1 Maximum cooling capacity..... | 78 |
| 4.2.1.1 Performance of the conventional type | 78 |
| 4.2.1.2 Performance of the loop type heat pipe..... | 85 |
| 4.2.2 Temperature uniformity | 96 |
| 4.3 Discussion | 111 |
| Chapter 5. Conclusion..... | 114 |
| References | 116 |
| Abstract in Korean | 122 |

List of Tables

| | |
|--|-----|
| Table. 1.1 Cooling technology for trains..... | 8 |
| Table 2.1 The specification of heat pipe | 36 |
| Table 3.1 Experiment case of optimal operation condition (refrigerant)..... | 65 |
| Table 3.2 Experiment case of optimal operation condition (quantity) | 66 |
| Table 3.3 Experiment case of performance analysis | 67 |
| Table 4.1 ΔT by the working fluid..... | 76 |
| Table 4.2 ΔT by the quantity of working fluid..... | 77 |
| Table 4.3 Experiment results of performance..... | 94 |
| Table 4.4 Temperature of each IGBT in conventional heat pipe | 99 |
| Table 4.5 Temperature of each IGBT in loop type heat pipe | 101 |
| Table 4.6 IGBT Temperature of heat pipe Type #2..... | 108 |
| Table 4.7 IGBT Temperature of Heat Pipe Type #3..... | 110 |

List of Figures

| | |
|---|----|
| Fig. 1.1 High-speed train development trend..... | 4 |
| Fig. 2.1 Conceptual diagram of conventional heat pipe | 17 |
| Fig. 2.2 Conceptual diagram of loop type heat pipe | 18 |
| Fig. 2.3 IGBT module to be installed on SIV stack..... | 21 |
| Fig. 2.4 Location of IGBTs on the SIV stack..... | 22 |
| Fig. 2.5 Figure of Merit by the working fluid | 25 |
| Fig. 2.6 Operation limits of heat pipe..... | 30 |
| Fig. 2.7 3D Modeling of conventional type (Type #1) | 37 |
| Fig. 2.8 Manufactured conventional type (Type #1)..... | 38 |
| Fig. 2.9 3D Modeling of loop type heat pipe (Type #2) | 40 |
| Fig. 2.10 Manufactured loop type heat pipe (Type #2) | 41 |
| Fig. 2.11 Heat Pipe for additional experiment (Type #3) .. | 42 |
| Fig. 3.1 Aluminum block for IGBT simulation..... | 45 |
| Fig. 3.2 Cartridge heater with aluminum block..... | 46 |
| Fig. 3.3 Power supply and VA meter | 47 |

| | |
|---|----|
| Fig. 3.4 Heat pipe with simulated IGBT module | 48 |
| Fig. 3.5 Wind tunnel and heat pipe | 50 |
| Fig. 3.6 Thermoelectric anemometer (MODEL 6162, KANOMEX) | 51 |
| Fig. 3.7 Vacuum pump with vacuum controller | 55 |
| Fig. 3.8 Heat pipe and fill valve on the reservoir | 56 |
| Fig. 3.9 Schematic of experiment | 57 |
| Fig. 3.10 The facility for the performance measuring | 58 |
| Fig. 3.11 Measuring points of temperature | 59 |
| Fig. 3.12 Measuring points of temperature (Type #2) | 60 |
| Fig. 3.13 Data Acquisition (DR 230, YOKOGAWA) | 61 |
| Fig. 3.14 VA meter (Model: PW3198, HIOKI) | 62 |
| Fig. 4.1 ΔT by the quantity of working fluid (FC-72) | 72 |
| Fig. 4.2 Temperature by the quantity of working fluid (water) | 73 |
| Fig. 4.3 ΔT by the quantity of working fluid (water) | 74 |
| Fig. 4.4 Performance comparison of 1600 cc and 1650 cc. | 75 |
| Fig. 4.5 IGBT temperature of conventional heat pipe (3 m/s, 2400 W) | 80 |

| | |
|--|----|
| Fig. 4.6 Conventional type ΔT (1 m/s forced convection) | 81 |
| Fig. 4.7 Conventional type ΔT (3 m/s forced convection) | 82 |
| Fig. 4.8 Conventional type ΔT (5 m/s forced convection) | 83 |
| Fig. 4.9 Performance of conventional heat pipe (Type #1)..... | 84 |
| Fig. 4.10 IGBTs temperature of loop type heat pipe (3m/s, 2400W) | 87 |
| Fig. 4.11 Loop type heat pipe ΔT (1m/s forced convection) . | 88 |
| Fig. 4.12 Loop type heat pipe ΔT (3m/s forced convection) . | 89 |
| Fig. 4.13 Loop type heat pipe ΔT (5m/s forced convection) . | 90 |
| Fig. 4.14 Performance of loop type (Type #2) | 91 |
| Fig. 4.15 Performance comparison of heat pipe #1 and #2 | 93 |
| Fig. 4.16 Maximum cooling capacity of heat pipe #1 and #2.. | 95 |
| Fig. 4.17 Temperature of each IGBT in conventional heat pipe | 98 |

| | |
|---|-----|
| Fig. 4.18 Temperature of each IGBT in loop type heat pipe | 100 |
| Fig. 4.19 Temperature of Type #1 (3 m/s, 3600 W) | 102 |
| Fig. 4.20 Temperature of Type #2 (3 m/s, 3600 W) | 103 |
| Fig. 4.21 Comparison of heat distribution..... | 106 |
| Fig. 4.22 Performance of Type #2 | 107 |
| Fig. 4.23 Performance of Type #3 | 109 |

Nomenclature

| | |
|------------|---|
| A | Area [m^2] |
| A_v | Vapor core cross section area [m^2] |
| A_w | Wick cross section area [m^2] |
| F_c | Flow friction coefficient of condensing [$(N/m^2)/W \cdot m$] |
| F_{cc} | Flow friction coefficient of compensation chamber [$(N/m^2)/W \cdot m$] |
| F_{sc} | Flow friction coefficient of subsidiary cooling unit [$(N/m^2)/W \cdot m$] |
| $F_{l,l}$ | Flow friction coefficient of liquid pipe [$(N/m^2)/W \cdot m$] |
| $F_{v,gr}$ | Flow friction coefficient of vapor groove pipe [$(N/m^2)/W \cdot m$] |
| $F_{v,l}$ | Flow friction coefficient of vapor pipe [$(N/m^2)/W \cdot m$] |
| F_w | Flow friction coefficient of wick [$(N/m^2)/W \cdot m$] |
| K | Wick permeability [m^2] |
| K_e | Effective thermal conductivity of wick [$W/m \cdot K$] |
| L | Effective heat pipe length [m] |
| L_e | Length of heat pipe evaporator [m] |
| M | Figure of Merit [W/m^2] |

| | |
|-----------------------|--|
| P | Pressure [N/m^2] |
| P_c | Capillary pressure [N/m^2] |
| $\Delta P_{c,max}$ | Maximum capillary pressure [N/m^2] |
| ΔP_l | Pressure drop in the liquid [N/m^2] |
| ΔP_v | Pressure drop in the vapor [N/m^2] |
| $\Delta P_{v,gr}$ | Pressure drop due to gravity [N/m^2] |
| Q | Thermal load [W] |
| R | Resistance of heat pipe [K/W] |
| R_v | Gas constant for vapor [J/kg·K] |
| Re | Reynolds number |
| T | Temperature [K] |
| T_v | Vapor temperature [K] |
| ΔT | Difference between $\Delta T_{max,IGBT}$ and T_{amb} [K] |
| T_{amb} | Ambient temperature [K] |
| $\Delta T_{max,IGBT}$ | Maximum temperature of IGBT [K] |
| We | Weber number |
| d | Diameter [m] |
| f | Coefficient of friction |
| h_{lv} | latent heat of vaporization [kJ/kg] |
| r | Radius [m] |
| r_c | Effective capillary radius [m] |
| r_{eff} | Effective pore radius [m] |

| | |
|----------|---|
| r_i | Inside radius of pipe [m] |
| r_n | Boiling nucleation radius [m] |
| r_v | Vapor core radius [m] |
| v | Velocity [m/s] |
| v_c | Limiting vapor velocity [m/c] |
| z | Dimension characterizing the vapor–liquid surface [m] |
| μ_l | Liquid dynamic viscosity [cP] |
| μ_v | Vapor dynamic viscosity [cP] |
| ρ | Density [kg/m^3] |
| ρ_l | Liquid density [kg/m^3] |
| ρ_v | Vapor density [kg/m^3] |
| σ | Surface tension coefficient [mN/m] |

Subscript

| | |
|-------------------|-----------------------------------|
| VCHP | Variable Conductance Heat Pipe |
| IGBT | Insulated Gate Bipolar Transistor |
| conventional type | Conventional heat pipe |
| loop type | Loop type heat pipe |
| LHP | Loop Heat Pipe |
| Tot | Total |
| cc | Compensation Chamber |
| amb | Ambient |
| CPL | Capillary Pumped Loop |
| DAQ | Data acquisition |

Chapter 1. Introduction

1.1 Background of the study

The train including high-speed railway has become a more important transportation in recent years as low-carbon, high-efficiency, and mass transportation systems. High-speed train is an eco-friendly transportation that emits lower carbon dioxide than that of a passenger car. Therefore, the demand for technology developments in high-speed train are expected to increase.

The type of train can be divided into centralized-power type and decentralized-power type according to the power device application method. The centralized-power type is a train in which a separate power device vehicle exists, and decentralized-power type is a train in which the power devices exist under each vehicle. Centralized-power type train do not have good acceleration, so they are advantageous for long-distance driving without stopping, and have the advantage of excellent ride quality in the cabin. However, there are disadvantages in that it is difficult to maintain the time interval between the trains in the operation where frequent stops are required. Also, there is a disadvantage of reducing the transport capacity due to the separated propulsion power devises vehicle. The main

advantage of decentralized-power type train is excellent acceleration, so it is suitable for subways or high-speed trains with frequent stops. It is known that decentralized-power type train has about 30% better acceleration and deceleration performance, and transport capacity than the centralized-power type train by the development of HEMU-430X which is one of decentralized-power type train. [1]

Due to the advantages of these decentralized-power type train, developed countries have been focused on the development of decentralized-power type trains to increase the speed of railways and increase the amount of transportation since the 2000s as shown in Figure 1.1. [2] In recent years, in consideration of energy efficiency, the development of high-speed train capable of reducing the shaft weight has been focused on decentralized-power type train. There is a case where the shaft weight was reduced from 17 tons to 14 tons through the distributed arrangement of the propulsion system. [3] In the case of South Korea, KTX and KTX-Sancheon, which are mainly used, are centralized-power type train, and in 2007, decentralized-power type train HEMU-430X began to be developed. The propulsion control system of train is a core technology, but with the recent development of power semiconductor and electronic circuit technology, core parts have been discontinued, increasing uncertainty in securing reliability. The application of IGBTs to the main circuit

switching elements of large-capacity propulsion control devices is becoming common as the development of electronic device technology. [4] IGBT has strong temperature characteristics and has an appropriate allowable temperature range. To keep the power converter at the operating temperature, a cooling devices capable of removing the heat released by the internal resistance is required. [5] The cooling method applied to the train is selected in consideration of the cooling capacity. The maximum thermal load of GTO Thyristor of normal train such as subway is about 800W, and in case of high-speed train with IGBT, it is around 1500~2000W. At low heat loads of less than 1000W, aluminum heatsinks using forced convection are mainly used as a cooling system. For loads higher than that, various cooling systems such as liquid (water) cooling type, heat pipe, phase changing type are used. [5]



Fig. 1.1 High-speed train development trend [2]

Table. 1.1 summarizes the various types of cooling systems by the train. The French Alstom TGV, the predecessor of KTX, uses submerge cooling system for cooling electric devices. It is a concept introduced as a phase change device since the 1970s and has been used until now. Submerge type cooling system is easy for large-capacity cooling by placing the element in a container. However, since the power semiconductor is immersed in the working fluid, maintenance is difficult. Although the structure of the cooler can be miniaturized, there is a disadvantage in that the weight of the cooler itself is heavy and the amount of working fluid required is large.[6]

Heat pipes were applied to South Korea KTX-Sancheon. The cooler consists of a VCHP with a block connected to the power semiconductor, and several fins installed on the condenser for radiating heat to the outside air. A working fluid which is excellent in the performance of heat transfer capability is injected into the pipe tube and vacuum is maintained. It transfers heat through the change phase of the refrigerant inside the container. Specifications of the heat pipe of the power converter currently used is a cooling capacity of 5 kW by forced convection in an environment of $-35 \sim 40^{\circ} \text{C}$. [6]

The traditional liquid (water) cooling system which has an excellent performance regarding reliability is applied to the KTX-Eum and HEMU-430X in South Korea. It consists of a pump for the working







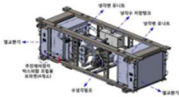
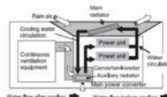
fluid circulating, a water-cooling plate and the cooling water, and a heat sink. The water-cooling system has disadvantages such as contamination of the pipe wall by antifreeze and an increase in maintenance cost due to leakage of coolant. [7]

In Japan, Shinkansen Fastec 360 uses water-cooling system. However, performance tests are being conducted on a method that uses a mixture of water cooling and phase change cooling. [4]

Although this disadvantage can be solved by a VCHP, a different type of it is needed. Because it should be installed in a limited space in a decentralized-power type train. Also, long-distance heat transport should be possible depending on the type of the train. In addition, in recent years, due to the discontinuation of electric devices like IGBTs of subway or high-speed rail that have been previously applied, there are cases where electric devices are replaced with elements having a thermal load equal to or greater than that of the existing ones. In this case, a cooler with improved cooling performance that should be installed in a predefined limited space is required, and at the same time, flexible arrangement of cooling device parts should be possible. A loop type can be the way to solve this problem. It has high density of cooling capacity with the ability to keep temperature uniform. It can also transport heat over long distances. There will be no entrainment limit as vapor and liquid flows separately. Comparing the performance

with conventional heat pipes by applying the loop type heat pipe to the IGBT modules of train is meaningful in that it presents a new cooling method for train IGBT with the improved cooling capacity.

Table. 1.1 Cooling technology for trains [6]

| | KTX ('02) | KTX-Sancheon ('10) | KTX-EUM, HEMU-430X ('12) | Japan-Shinkansen ('07) |
|------------------|---|---|---|--|
| Train |  Centralized-power Type |  Centralized-power Type |  Decentralized-power Type |  Decentralized-power Type |
| Cooling Type |  Liquid(water) Cooling |  Conventional Heat Pipe |  Liquid(water) cooling |  Evaporative cooling |
| Charac-teristics | Submerge of semiconductor, Heavy due to the amount of working fluid | Reliability, Limitation of space | Reliability, Dew condensation, Leak of working fluid, Environmental issues by the leak of fluid | Leak of working fluid |

1.2 Literature review

1.2.1 Cooling of electric devices method

Liquid cooling system, air type chiller, evaporative cooling system and heat pipes are applied for cooling IGBTs or electric devices in high-speed rail or subway. Before studying the loop heat pipe as a cooling method to increase space efficiency, investigations of recent research cases related to cooling of IGBTs, or electric devices and the effects on it were conducted.

Lee et al. [8] proposes a heat pipe design technology, such as the length ratio of the evaporation and condensing parts, and the injection amount of the working fluid for cooling semiconductors for subway vehicles. For heat transport of 300 W per unit, a pipe with a diameter of 15.88 mm was suitable. When the length ratio of the evaporator and the condensing part is 3.5 or more, the appropriate range of the refrigerant is determined to be 80% to 90%. Cho et al. [9] studied the suitability and commercialization of a crossflow plate heat exchanger to maintain a 10 kW-class power conversion semiconductor within the allowable temperature range of 100 °C. In conclusion, thermal load of 10 kW can be cooled by water cooling system with the coefficient of about 2500~3000 W/m²K. Xavier Perpiñà et al. [10] analyzed the

effect of non-uniform heat distribution inside the IGBT module on the reliability of the railway power inverter and the effect of thermal cycle on the components of the IGBT module. And it was found that the non-uniform temperature distribution at the package level causes the failure of the IGBT module due to overheating. Lee et. al [11] studied the heat pipe design processes in order to get a reliability of the power devices in a railway propulsion system. Four design methods were suggested over 20-year lifetime which is the requirements in the train industry with an accuracy of 80% or more for junction temperature.

1.2.2 Loop heat pipe as a cooling system

LHPs and CPLs were introduced to improve the performance in the case of a heat pipe which is applied a long pipe with wicks and small pore radius. [12] Stenger [13] suggested CPL in 1966. The first loop heat pipe was developed by Maydanik [14] in 1972. The development of it was due to the possibilities to be applied in space. As a cooling system in space, it is required high transport capacity.

Jentung Ku et al. [15] analyzed the temperature fluctuation that can be found under certain conditions with the temperature never converge. And confirmed that the temperature oscillation of the

condensed liquid causes the temperature fluctuation of cc and the fraction fluctuation of void inside the evaporator core. Zhang Hongxing et al. [16] researched the effects regarding the startup of operation and correlation the startup with the steady-state operation of LHPs. It has been found that the increase of the pressure leading to condensation of the refrigerant in CC, as well as heat leakage from the evaporator to CC, causes the temperature of CC to rise during start-up. Tarik Kaya et al. [17] established numerical model of the capillary porous structure of LHP regarding the heat and mass transfer with boiling limit. It is confirmed that in order to enhance the limitation of cooling performance related to boiling, it is recommended to maintain good contact at the pin-wick interface with the removal of non-condensable gases. Shane Storrington [18] designed and manufactured three LHPs and presented a detailed development process including initial design criteria like materials of pipe, assembly, fluid filling, and sealing. After optimizing the conditions of fluid inventory, the LHPs were able to start and operate reliably in a power load range of 5 to 55 W. Ki [19] studied a loop heat pipe test model for the power conversion semiconductor applied to high-speed rail. LHP start-up stability was confirmed at a relatively low heat load, and the resistance was 1.052~1.62 °C/W at a thermal load of 50W. Lizhan Bai et al. [20] studied a mathematical model of steady-state

LHP and analyzed it using experimental data. Presented the results of distribution of pressure drop, influence of the temperature of sink. Xianbing Ji et al. [21] designed and investigated LHP regarding the wicks with composite multiscale porous to study cooling performance and start-up features. The composite multiscale porous wicks reduced the time of start-up, lowered the temperature of pipe wall, and the temperature fluctuation. At a thermal load of 200 W, the loop type had a wall temperature of 63°C and reached a $40W/cm^2$. Ainur Rosidi et al. [22] simulated heat transfer and flow characterization phenomena in a wickless LHP. This simulation study provided the results of the influence of evaporator charging ratio and thermal load in LHP. In the case of a 80% charging ratio and an evaporator thermal load of 55° C was applied, natural circulation flow was possible after 1000 seconds passed when the working fluid reached the saturation temperature.

1.3 Purpose and scope

As the use of electronic devices increases in various fields, there are demands to improve the cooling capacity per unit volume in industrial fields such as high-speed train and energy storage systems. This study proposes a loop type heat pipe that can replace the conventional

heat pipe as a way of improving the cooling capacity per unit volume, A loop type is more advantageous than a conventional one in terms of long-distance heat transport, enabling efficient arrangement of cooling devices and increasing space efficiency. In addition, greater heat can be transferred by reducing the resistance between the movement of the heated gas and the liquefied working fluid. The goal of this study is to experimentally analyze the performance difference between a loop type and a conventional type.

A conventional type and a loop type having a similar structure were designed and manufactured to experimentally confirm the performance. Conventional heat pipe system was manufactured with 14EA single tube heat pipes with groove type wick structure. Loop type heat pipe was manufactured by reflecting operating limits in Chapter 2, and compatibility of working fluid and material for stable steady-state operation.

In Chapter 3 and Chapter 4, the performances of the conventional type and the loop type were compared through the experiment. For the newly applied loop type, the optimal operating conditions for the refrigerant were suggested by comparing the performance regarding the type and the amount. The performance comparison of each heat pipe was made in terms of maximum cooling capacity with thermal resistance and temperature uniformity of the IGBT module. Forced

convection was applied by the wind tunnel to simulate the railway operating conditions, and the IGBT was simulated using VA meters with power supplies. Experimental results of the conventional type and the loop type heat pipe were compared and analyzed by calculating the maximum cooling capacity and the temperature uniformity in the IGBT module depending on the degree of forced convection and the thermal load.

Chapter 2. Design and manufacture

2.1 Concept design

Heat pipe applied for cooling the train SIV stack is generally in the form of a simple tube with an internal wick structure. When thermal load is affected to the evaporator located in the heating element, the refrigerant is vaporized and moves inside the tube to reach the condenser. In the condenser part, several fins are generally installed for efficient heat transfer, and the working fluid is liquefied after cooling. The wick inside the heat pipe generates a capillary force that can move the liquid refrigerant back to the evaporator. As a result, the continuity of operation is ensured, and the refrigerant circulates in the pipe. The conceptual diagram of the conventional type is shown in Figure 2.1.

To enhance the space efficiency, the loop type was applied in this study with a separate pipe return line to return the refrigerant from the reservoir of condenser to the reservoir of evaporator. Due to the separate return pipe, the movement of the liquefied refrigerant does not act as a resistance to the movement of the steam generated in the evaporator, so the cooling performance will be improved. The conceptual diagram of the loop type is shown in Figure 2.2.

In the conventional type, several separated heat pipes in the form of a single tube were press-fitted parallel to one aluminum plate to form one system. Both ends of each single heat pipe are sealed with endcaps, and the refrigerant of each pipe is completely separated. Since loop type heat pipe should be formed as one system, connecting parts to connect each single heat pipe are required. In Figure 2.2, there are two reservoirs connecting each heat pipe. One is located under the condenser to collect the liquefied refrigerant, and the other is located at the top of the evaporator so that the steamed refrigerant passes. The steamed refrigerant moves through a single return pipe.

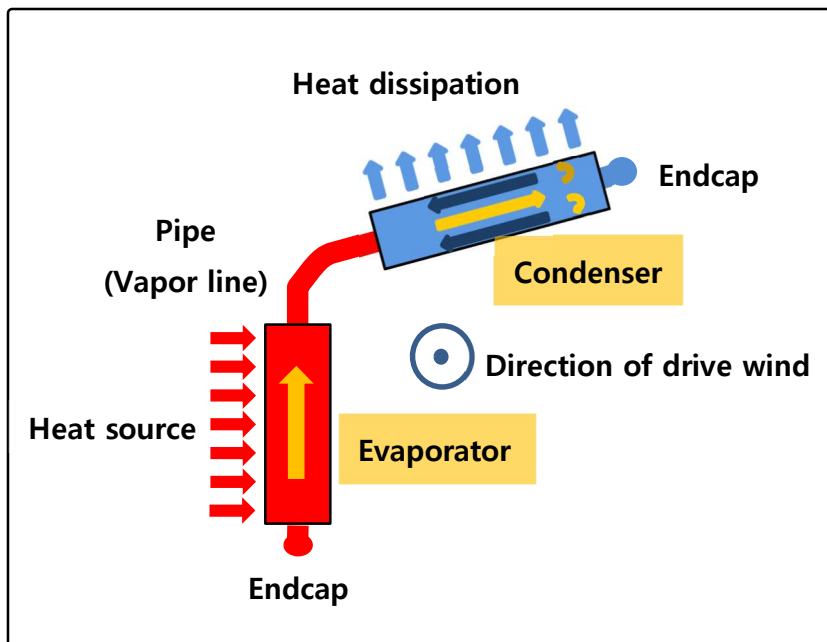


Fig. 2.1 Conceptual diagram of conventional heat pipe

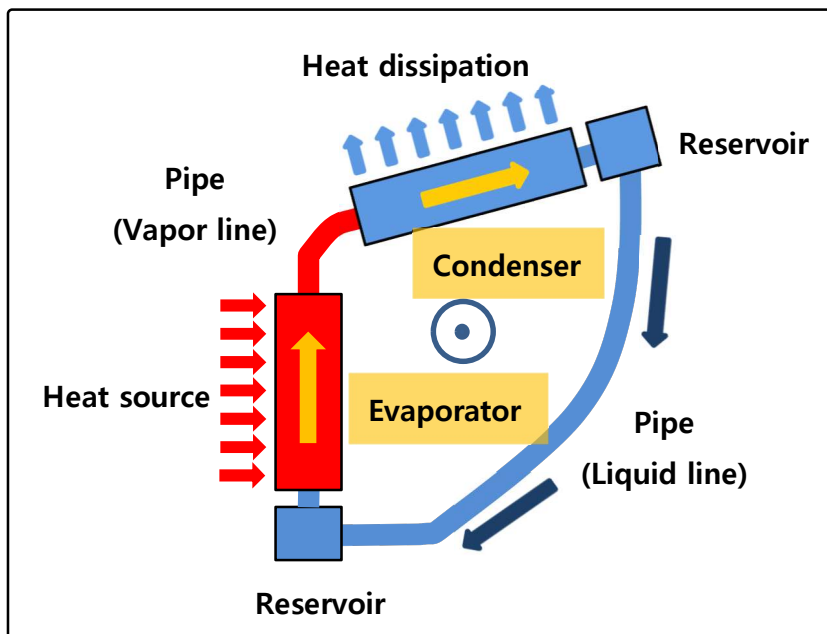


Fig. 2.2 Conceptual diagram of loop type heat pipe

2.2 Element Design

Element design was carried out in consideration of target specifications such as installation space, cooling capacity, and operation limits.

2.2.1 Target specification

The heat pipe applied in this study is used to cool the IGBT module of the subway or high-speed rail SIV stack. This study is aimed at cooling the IGBT module shown in Figure 2.3, which typically generates 800 W of heat per unit. A total of 3 IGBTs are installed in the subway SIV Stack with the total amount of heat 2400 W. Three IGBTs are placed on the base plate as shown in Figure 2.4. The space allowed for cooling module is $925 \times 630 \times 633.5$.

The main performance used in the train is ΔT and the thermal resistance R . The ΔT is defined as equation 2.1.

$$\Delta T = T_{max,IGBT} - T_{amb} \quad (2.1)$$

The maximum cooling capacity can be determined by the allowable value of ΔT . The maximum allowable value of ΔT suggested by

the railway company is 60° C in consideration of the reliability of IGBT module.

At a heat source of 2400 W, ΔT should be less than or equal to 60° C.

Total thermal resistance can be calculated by equation (2.2).

$$R_{\text{tot}} = \frac{T_{ho} - T_{cold}}{Q} \quad (2.2)$$

The maximum allowable thermal resistance R should be lower than 0.025 K/W in this study. The heat pipe used in the study is installed on the train and is affected by the driving wind. The SIV stack applied to the subway is usually 3 m/s in many cases, so the above target specification should be satisfied in the 3 m/s driving wind environment.



Fig. 2.3 IGBT module to be installed on SIV stack



Fig. 2.4 Location of IGBTs on the SIV stack

2.2.2 Refrigerant and pipe

2.2.2.1 Refrigerant

It is recommended that the operating temperature of the IGBTs of the subway SIV Stack used in this study be kept below 120 °C. Therefore, in this study, it is necessary to select a working fluid that is mainly applied to relatively low-temperature heat pipes. In addition, to maximize the performance of the heat pipe, it is necessary to select the refrigerant considering the Figure of Merit. Figure of Merit M is expressed as equation 2.3. [23]

$$M = \frac{\rho_l \sigma h_{lv}}{\mu_l} \quad (2.3)$$

With the given Figure of Merit, the maximum heat transfer amount is expressed as the equation 2.4 [26].

$$(QL)_{c,max} = 2 \left(\frac{\sigma \rho_l h_{lv}}{\mu_l} \right) \left(\frac{K}{r_c} \right) A_w \quad (2.4)$$

Therefore, the amount of heat transfer increase as the Figure of Merit increase. Figure 2.5 shows the Figure of Merit by the working fluid.

According to N.Dunbar and P.Cadell , in case of loop heat pipe, Figure of Merit changed as Equation 2.5. [25]

$$M = \frac{\rho_v h_{lv}^{7/4} \sigma}{\mu_v^{1/4}} \quad (2.5)$$

This difference is known to occur because the vapor line flow in the LHP is generally turbulent, and the vapor pressure drop is dominant. [23] Considering the Figure of Merit of conventional type and loop heat pipe, the suitable working fluids for this study are water and ammonia. However, due to the useful range of the working fluid, water is the most suitable working fluid.

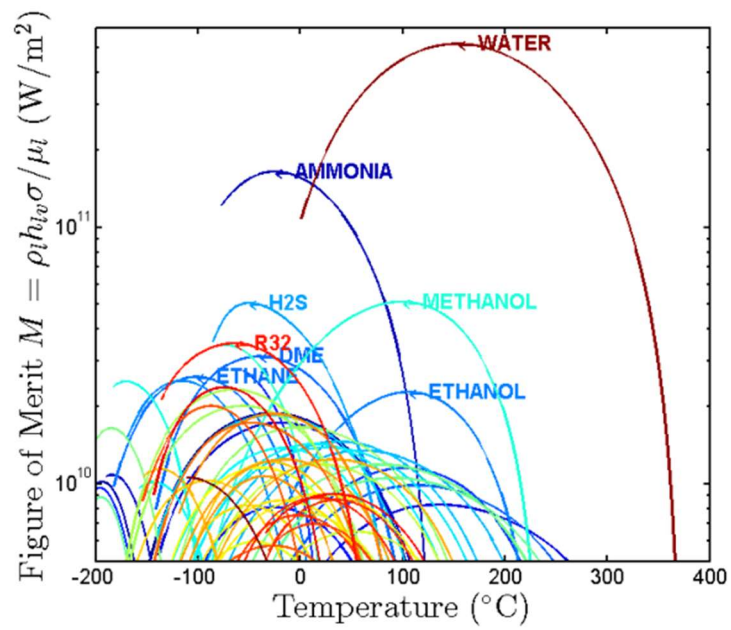


Fig. 2.5 Figure of Merit by the working fluid [25]

2.2.2.2 Specification of pipe

Compatibility between the refrigerant and the material is the most important. The compatibility of the refrigerant and the container material affects the problems such as corrosion and erosion caused by chemical reactions and the production of non-condensable gas, which can result in fatal consequences for the performance of the heat pipe. In addition, the weight, tensile strength, and thermal conductivity of the material are taken into consideration. [24] In consideration of compatibility with water, excellent thermal conductivity, and economic feasibility, the material was decided to be copper.

To determine the diameter of single pipe tube, Mach number should be considered. Mach number of the steam should not exceed 0.2. Reflecting this, the minimum inner diameter to be selected should be larger than this. [24]

$$d_v = \left(\frac{20Q_{\max}}{\pi \rho_v h_{lv} \sqrt{\gamma_v R_v T_v}} \right)^{\frac{1}{2}} \quad (2.6)$$

Considering this and the space that can be attached to the SIV Stack, it was decided to use the standard copper pipe of Ø15.88 for heat pipe production. According to the ASME code, the maximum allowable

stress when designing a pipe container that withstands vapor pressure is stipulated as 25% of the ultimate tensile strength. [24] This copper tube can withstand a maximum pressure of 74.5 Mpa, so there is no problem in applying it to heat pipe production.

2.2.2.3 Wick structure

Wick is installed on the inner wall of each pipe tube to generate capillary force. A screen wick, groove wick, sintered metal wick, etc. can be used as wick structure. In some cases, a combination of various types of wicks can be installed. In order to increase heat transfer, high permeability of the wick is required, while in order to induce large capillary force, the smaller capillary radius is advantageous. Groove type wick has the disadvantage of having a large capillary radius, but considering the economic feasibility, it has very good mass productivity. [26] In this study, considering the possibility of expansion and distribution, the most economical triangular groove type was applied. When the target performance was not achieved with the groove type wick, another type of wick will be considered.

2.2.3 Operation limits

Continuous operation may not be possible under certain operating conditions, which is affected by the operating limit. The possible areas of the limitations are shown in Figure 2.6. [28]

2.2.3.1 Capillary limit

As in this study, the most likely and important limitation in the low temperature range is the capillary limit. The total pressure loss which is required for the refrigerant to circulate the loop increases as the magnitude of the mass flow rate increases. This value should be lower than the maximum capillary pressure that can be generated at the steam–liquid interface of the wick. [27] This can be expressed by Equation (2.7).

$$\Delta P_{c,max} \geq \Delta P_{tot} = \Delta P_{v,gr} + \Delta P_v + \Delta P_l \quad (2.7)$$

Due to a curved liquid surface, there are pressure differences. If the surface is not spherical with two radii r_1 and r_2 , then pressure difference can be calculated by the Equation (2.8). [27]

$$\Delta P_c = \sigma \left(\frac{1}{r_1} + \frac{1}{r_2} \right) \text{ (Young – Laplace equation)} \quad (2.8)$$

Through the equation (2.9), the maximum capillary pressure is obtained from the microstructure of a given wick. [27]

$$\Delta P_{c,\max} = \frac{2 \sigma}{r_{\text{eff}}} \cos \theta \quad (2.9)$$

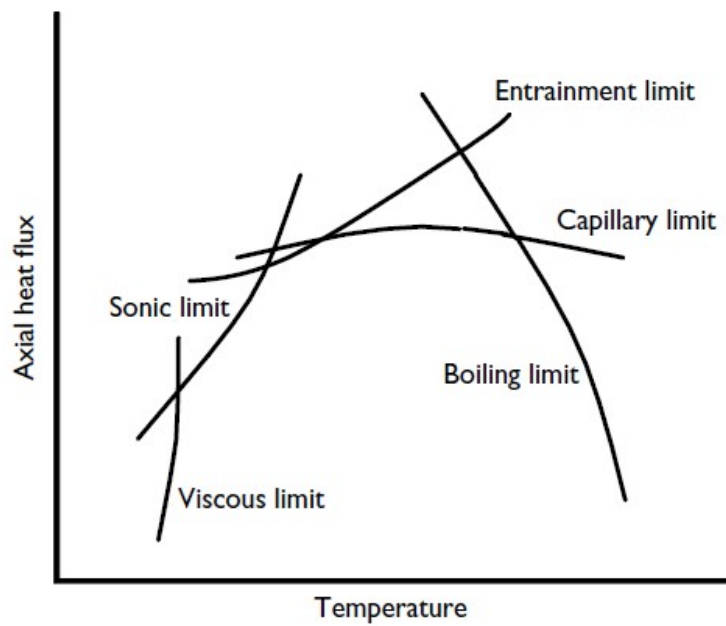


Fig. 2.6 Operation limits of heat pipe [28]

2.2.3.2 Boiling limit

It refers to a case in which the operation is restricted because the bubbles generated by boiling in the liquid return path impede the axial flow of the liquid. In general, it can be calculated with the following equation (2.10). [29]

$$Q_{b,max} = \frac{2 \pi L_e K_e T_v}{\lambda \rho_v \ln\left(\frac{r_i}{r_v}\right)} \left(\frac{2 \sigma}{r_n} - P_c \right) \quad (2.10)$$

However, in the open groove type among groove wicks, it is not applicable because the vapor generated by the open groove gap can be discharged to the vapor area. The calculation results are for the reference only.

2.2.3.3 Sonic limit

It is an operating limit that is considered when given a heat flux large enough that the vapor velocity at the end of the evaporator reaches the sonic velocity. Sonic velocity at the end of the evaporator can be expressed by equation (2.11). [29]

$$M_v = \frac{Q}{A_v \rho_v h_{lv} \sqrt{\gamma_v R_v T_v}} \quad (2.11)$$

The maximum heat transfer is expressed as the following equation (2.12). [29]

$$Q_{s,max} = A_v \rho_v h_{lv} \left[\frac{r_v R_v T_v}{2(r_v + 1)} \right]^{1/2} \quad (2.12)$$

The sonic limit is usually very large for low-temperature heat pipes, so it can be said that there is no practical problem. If the diameter of vapor flow path is too small, it may be a problem, but in this study, it is not applied by using a copper tube of Ø15.88.

2.2.3.4 Entrainment limit

Inside of the pipe tube, the vapor flows from the evaporator to the condenser and the liquid is returned by the wick. [30] This entrainment could be acted as resistance by the surface tension. [30]

Kim and Peterson studied and defined the Webber number that can determine the occurrence of entrainment. [31]

$$We = \frac{\rho_v v^2 z}{\sigma_l} \quad (2.13)$$

In (2.13), z is the variable regarding the space of wick.

Entrainment may occur when We is of the order 1. [30] The limiting vapor velocity, v_c , is calculated by equation (2.14).

$$v_c = \sqrt{\frac{2\pi\sigma_l}{\sigma_v z}} \quad (2.14)$$

Thus, the maximum axial flux is shown in the equation (2.15).[30]

$$q = \sqrt{\frac{2\pi\rho_v h^2 \sigma_l}{z}} \quad (2.15)$$

However, Entrainment limit is less important in the low-temperature heat pipe

2.3 Manufacture of heat pipe

A total of three heat pipes were manufactured by reflecting the concept design, working fluid, pipe selection results and operation limit. A conventional one (Type #1) and a loop type (Type #2) for the main experiment were manufactured, and one more new type (Type #3) for additional experiments was manufactured, respectively. Table 2.1 summarizes the specifications of the manufactured heat pipe. They have the same size as $560 \times 510 \times 560$ including external frame, which satisfies the condition that it should be within $925 \times 630 \times 633$.

The 3D modeling result of the conventional type is shown in Figure 2.7. A total of 14EA $\varnothing 15.88$ copper single tube heat pipes are press-fitted into a 25 mm-thick main aluminum plate to constitute a system. The interval of each single pipe was set to be about 30 mm. For efficient space utilization, heat pipe single tubes are bent. The bending angle was set to over 90° so that the working fluid liquefied in the condenser could effectively return to the evaporator with the help of gravity. The lengths of the evaporator and condenser of all pipes are the same length of 330 and 424 mm, respectively, but the total length of the pipe is different as shown in Figure 2.7. Consists of 8 pipes marked in green and 6 pipes marked in red, and this is to increase the

strength of the fin installed in the condenser. A total of 44 fins were installed with a size of 560 x 220 x 1t. The manufactured conventional heat pipe is expressed in Figure 2.8.

Table 2.1 The specification of heat pipe

| Type of Heat pipe | | #1 | #2 | #3 |
|-----------------------|------------|-------------------|----|----|
| Container Material | | Copper | | |
| Outer Diameter | | Ø15.88 | | |
| Inner Diameter | | Ø14.08 | | |
| Length | Evaporator | 330 | | |
| | Condenser | 424 | | |
| No of reservoir | | 0 | 2 | 1 |
| No of retrun line | | 0 | 1 | 0 |
| Geometry of Wick | | Groove | | |
| Target Resistance | | 0.025 | | |
| Target Size of Module | | 925 × 630 × 633.5 | | |
| Refrigerant | | Distilled Water | | |
| Fill Charge Ratio | | 30% or more | | |

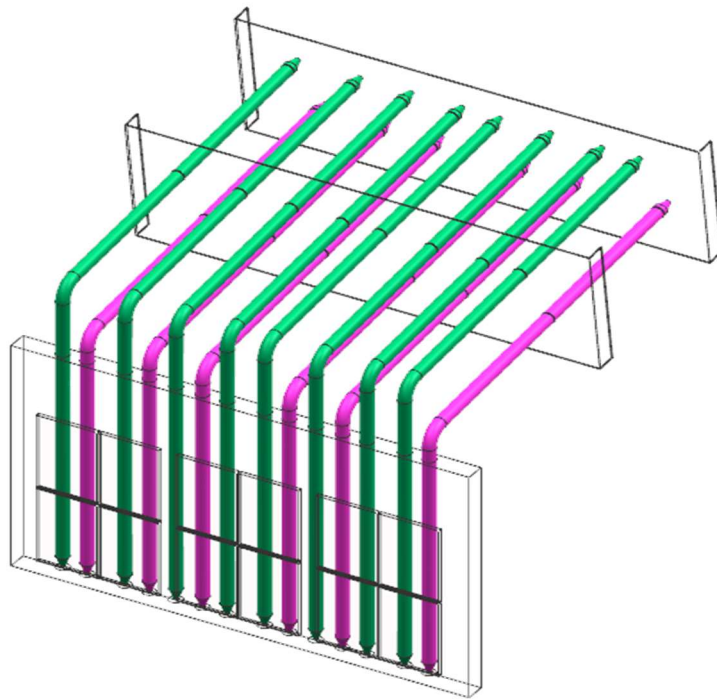


Fig. 2.7 3D Modeling of conventional type (Type #1)

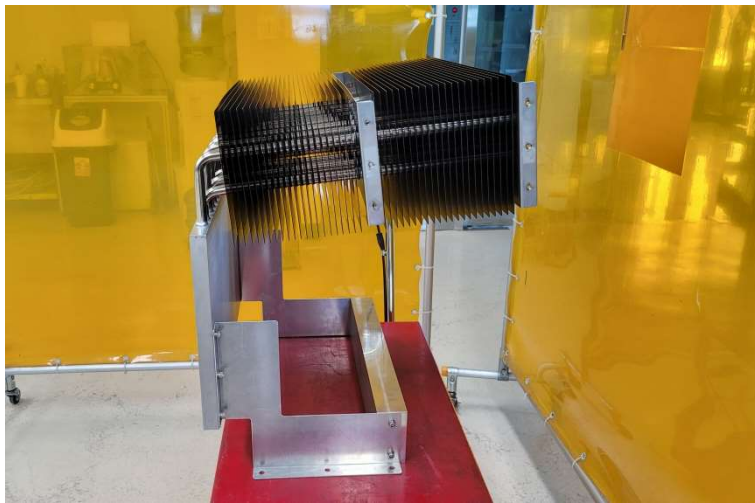


Fig. 2.8 Manufactured conventional type (Type #1)

Most of the parts of the loop type were manufactured similarly with the conventional type so that the effect of the loop could be experimentally compared in the performance comparison. The sizes of Ø15.88 14 EA copper tubes, main plate, evaporator, and condenser are the same. The difference is 2 reservoirs and 1 return pipe, which can be seen in the 3D modeling of the loop type in Figure 2.9. In the figure, two reservoirs are marked in orange, and the return line is marked in red. The two reservoirs connect each single pipe tube to form a loop type system. The size of the reservoir located at the bottom of the evaporator is 560 x 110 x 110, and the size of the reservoir located at the top of the condenser is 560 x 110 x 150. The manufactured loop type is shown in Figure 2.10.

Figure 2.11 shows the heat pipe type #3 which is additionally manufactured to analyze the effect of reservoir on the IGBT module temperature distribution. The shape is the same as that of a conventional heat pipe, and single pipe tubes are connected to one reservoir at the bottom of the evaporator. Since there is no separate reservoir at the top of the condenser, it does not form a loop.

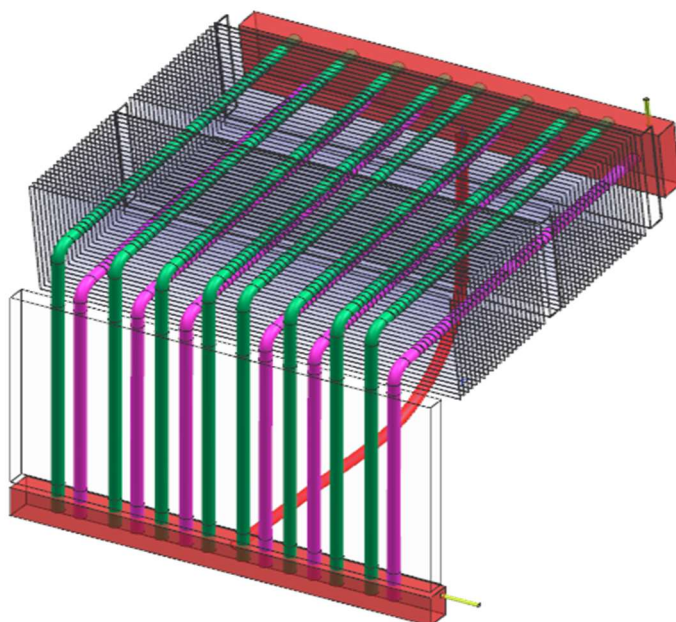


Fig. 2.9 3D Modeling of loop type heat pipe (Type #2)

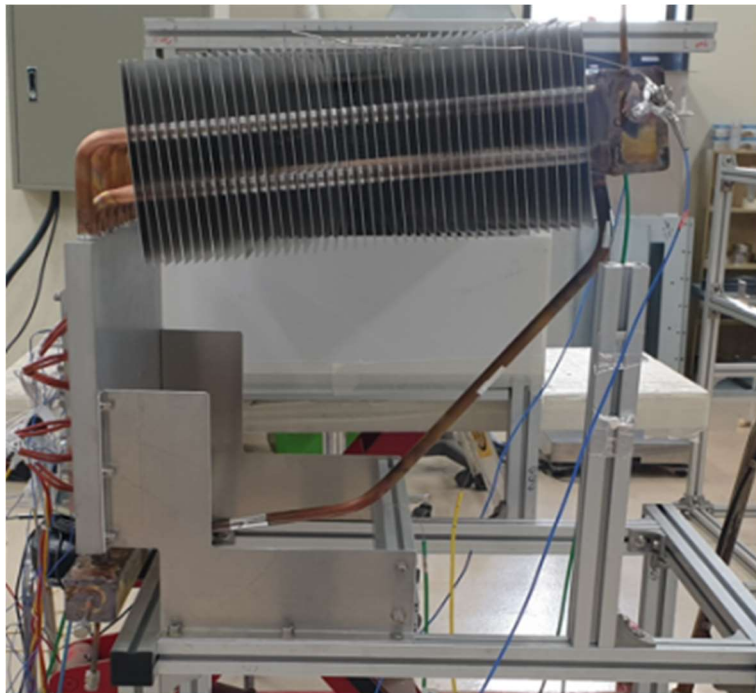


Fig. 2.10 Manufactured loop type heat pipe (Type #2)

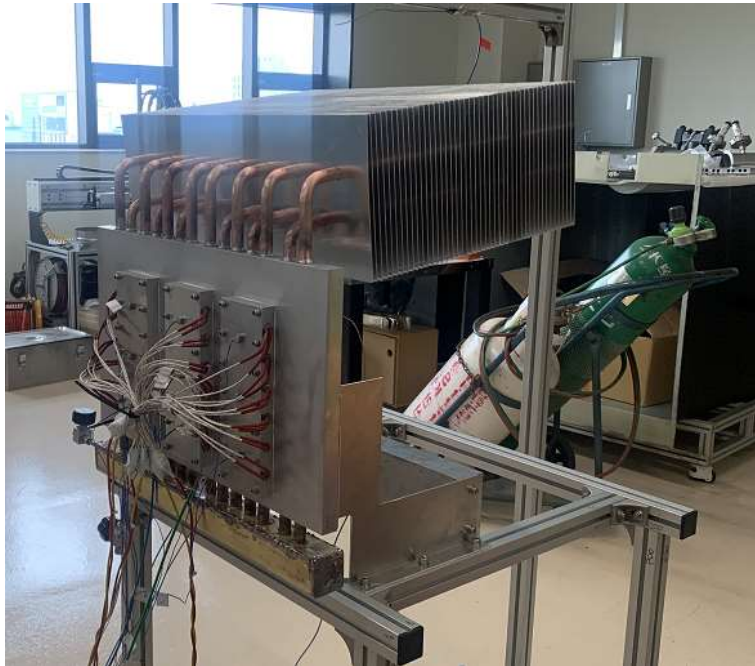


Fig. 2.11 Heat Pipe for additional experiment (Type #3)

Chapter 3. Experimental setup and facility

3.1 Simulation of environment

3.1.1 Simulation of IGBT module

Three IGBTs of size $89 \times 250 \times 19$ are attached to the SIV Stack of size $925 \times 630 \times 633.5$, and base thermal load of each IGBT module is 800 W, respectively. To simulate the same heat characteristics as the IGBT module, three aluminum blocks of the same size were manufactured as shown in Figure 3.1. Heat was simulated with a cartridge heater, and a total of 6 cartridge heaters were applied per block as shown in Figure 3.2. Cartridge heaters can generate maximum 250 W of heat per unit, so a maximum of 1500 W of heat per block can be applied. Cartridge heaters were installed in blocks at around 30 mm intervals. Heat is supplied by the power supply, and for thermal load control, the VA meter (PW3178, HIOKI) shown in Figure 3.3 was used. To measure the performance of conventional type and loop type in various cases, the total thermal load was made from 1800 W to 4500 W.

To facilitate heat transfer from the simulated block to the stack, the IGBT module simulated by aluminum block and main plate of heat pipe

module were attached using a conductive compound (G-747, ShinEtsu). Finally, the SIV Stack and simulated IGBT modules installed are shown in Figure 3.4.

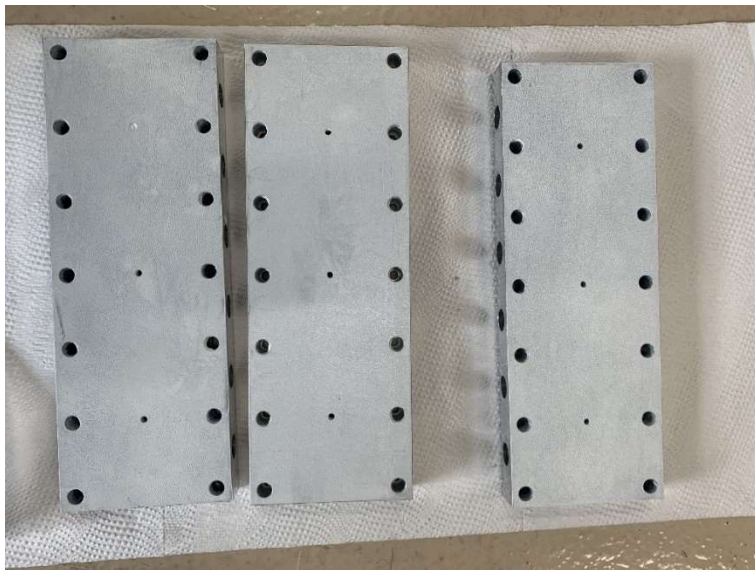


Fig. 3.1 Aluminum block for IGBT simulation

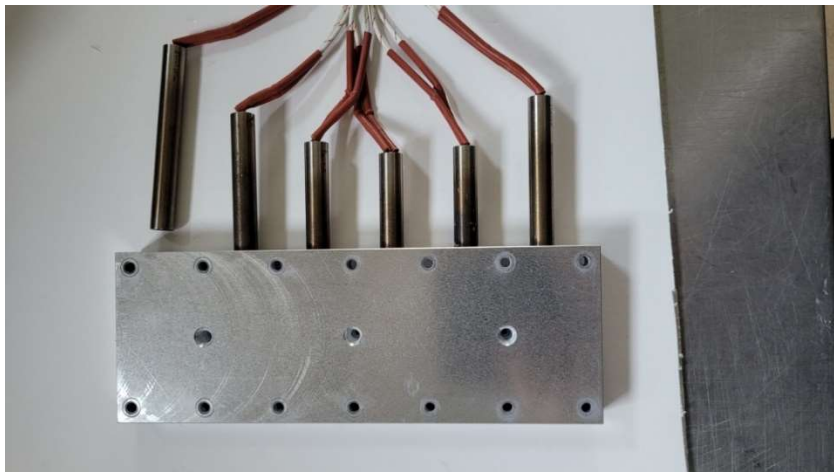


Fig. 3.2 Cartridge heater with aluminum block

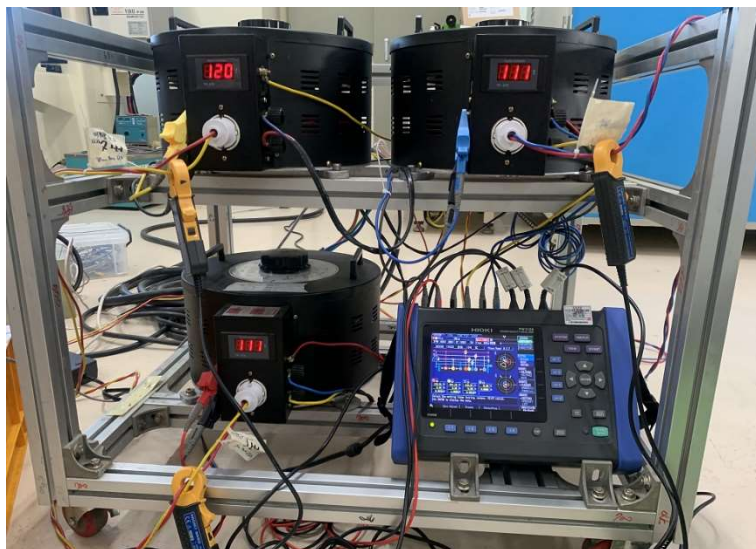


Fig. 3.3 Power supply and VA meter

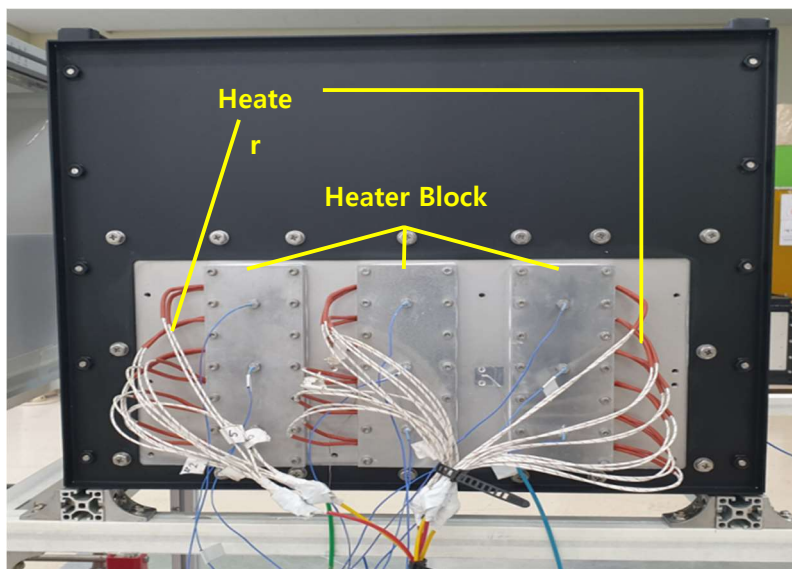


Fig. 3.4 Heat pipe with simulated IGBT module

3.1.2 Operating environment simulation

IGBT module of SIV Stack is applied to subway or high-speed rail, so cooling is required while driving. Therefore, the IGBT module is affected by the driving wind and the wind speed of the driving wind varies depending on the driving characteristics of the train.

Considering the air flow into the IGBT module while driving, the experiment was conducted for three driving winds of 1 m/s, 3 m/s and 5 m/s. The standard wind speed suggested by the railroad company is 3 m/s. The driving wind was simulated with a wind tunnel as expressed in Figure 3.5. In consideration of the driving direction, a heat pipe was installed so that the running wind flows along the heat pipe condenser fins. The experiment was conducted in an enclosed space so as not to be affected by convection other than the driving wind. The wind speed was measured using the thermoelectric anemometer (MODEL 6162, KANOMEX) shown in Figure 3.6. The thermoelectric anemometer measures the wind speed within 50 m/s with a measurement unit of 0.01 m/s, and the measurement error is 0.15 m/s.

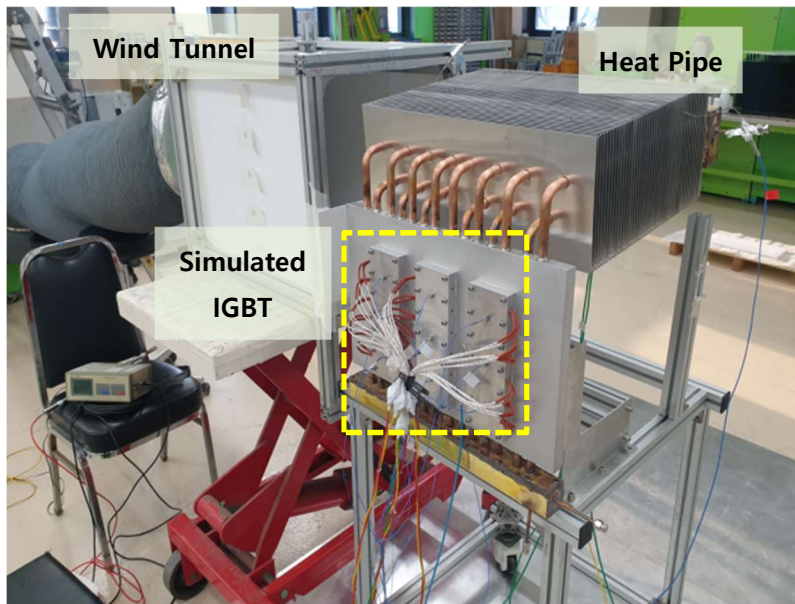


Fig. 3.5 Wind tunnel and heat pipe



Fig. 3.6 Thermoelectric anemometer
(MODEL 6162, KANOMEX)

3.2 Experimental setup

3.2.1 Setup of heat pipe

In order to conduct experiment, it is necessary to inject the refrigerant and maintain the internal vacuum. If there is an air in the heat pipe and it is not a vacuum state, the heat pipe performance will be deteriorated, making accurate performance testing impossible. A vacuum pump as shown in Figure 3.7 was used to create a vacuum after injecting working fluid into the pipe tube. Vacuum pump is a diffusion oil type, and XGS-600 (Varian) and KVC were used as vacuum controllers. For extraction using a vacuum pump, a separate fill tube and valve were installed on the reservoir above the heat pipe condenser as shown in Figure 3.8. When the refrigerant was injected, the internal air was extracted 5 times or more to lower the internal pressure to 0.001 bar. 0.001 bar is a low pressure that can be obtained by using a vacuum pump of Figure 3.7, and it can be considered that a vacuum state is achieved when the pressure is achieved.

3.2.2 Experiment facility

The schematic of experiment for the performance test is expressed in Figure 3.9 and Figure 3.10. A heat pipe was installed to connect with the wind tunnel to simulate the driving wind effect by forced convection. The speed of the driving wind was measured and controlled with a thermoelectric anemometer every 4 seconds.

The temperatures of the IGBTs were measured every 2 seconds using a thermocouple, and the measured data was collected through DAQ. The heat of the simulated IGBT module is supplied through the cartridge heater, and it is controlled by the power supply and VA meter. Figure 3.10 is the picture of installed facility.

Temperature was measured using K-type thermocouple. The location of temperature measurement points (maximum 17 points) in the IGBT Module is shown in Figure 3.11 and Figure 3.12.

Temperatures were measured at three points in each of IGBTs #1, #2, and #3. The temperature between each IGBT was also measured for the reference. To calculate the cooling capacity of each heat pipe ΔT , the air inlet, outlet points of the wind tunnel, and the air temperature above and below the heat pipe were measured separately. In the case of the loop type, as expressed in Figure 3.12, the temperature of reservoirs and return line were measured to check

whether the loop type heat pipe was operating correctly. The temperature data measured every 2 seconds were collected using the DAQ (DR 230, YOKOGAWA) in Figure 3.13.

The VA meter is composed of three channels as shown in Figure 3.14 so that the thermal load of the three IGBTs attached to the heat pipe can be adjusted respectively. Each channel controls one IGBT thermal load, and the maximum thermal load is 1500W per channel.



Fig. 3.7 Vacuum pump with vacuum controller

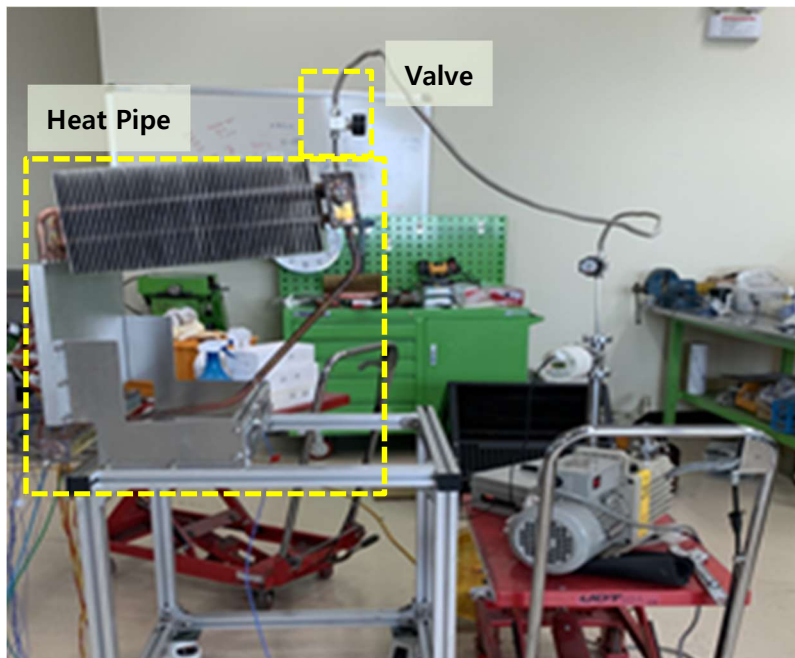


Fig. 3.8 Heat pipe and fill valve on the reservoir

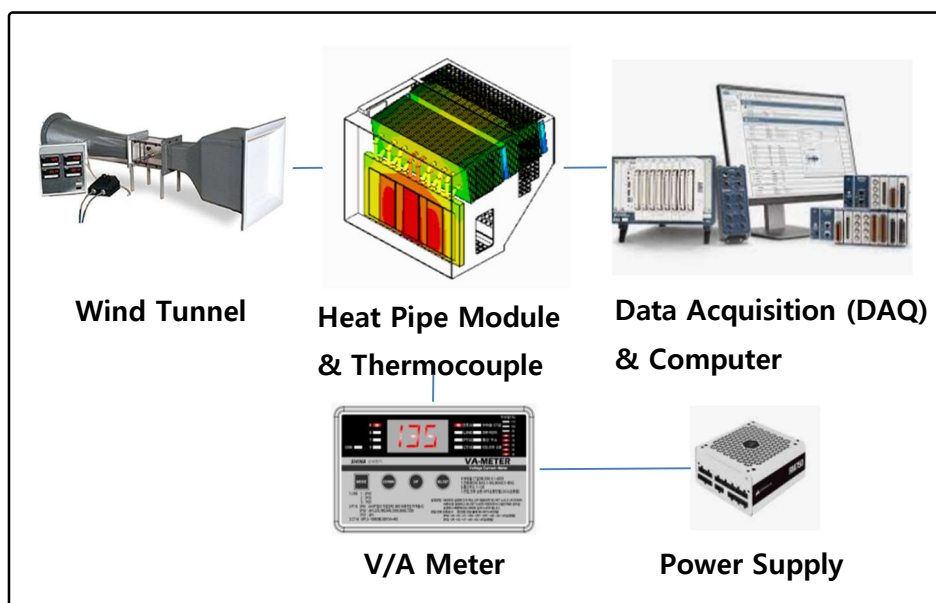


Fig. 3.9 Schematic of experiment



Fig. 3.10 The facility for the performance measuring

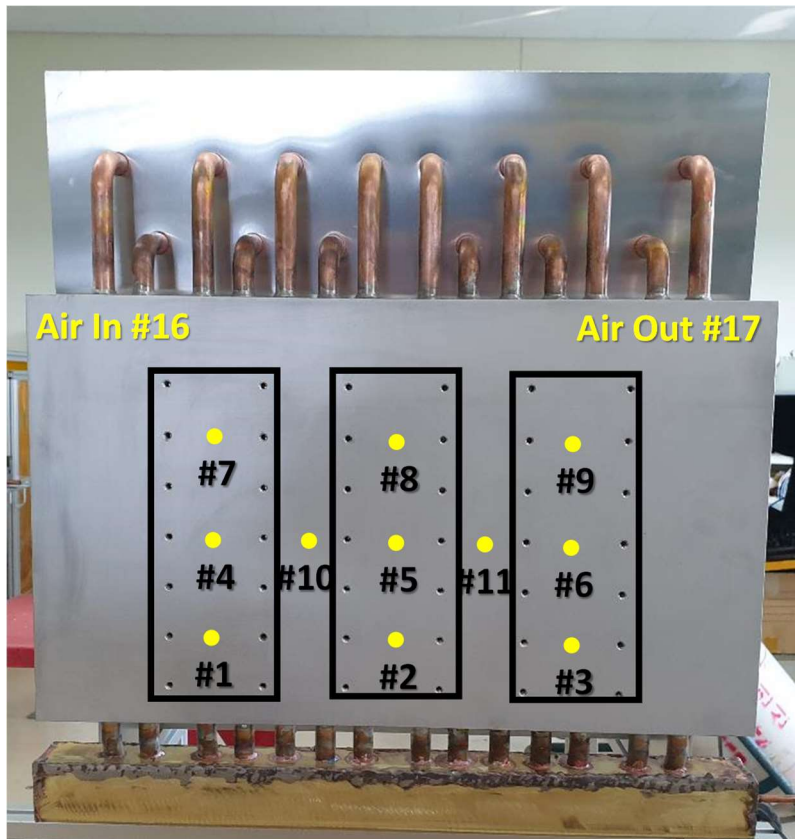


Fig. 3.11 Measuring points of temperature

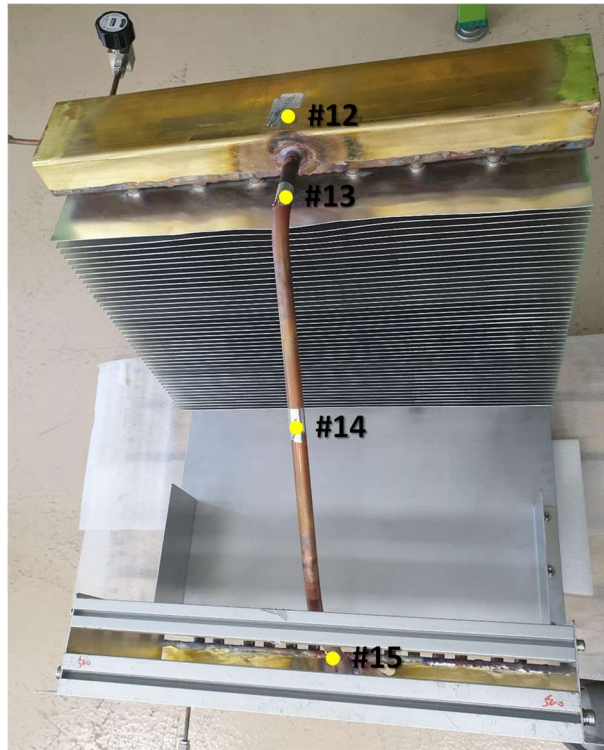


Fig. 3.12 Measuring points of temperature (Type #2)

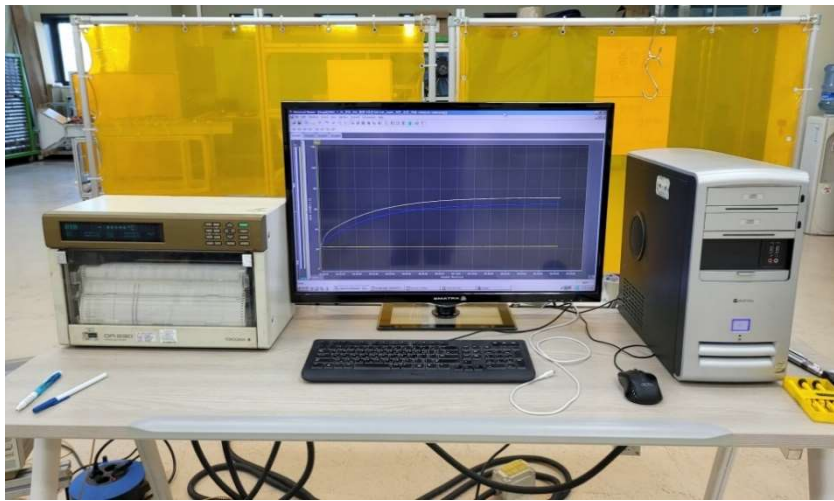


Fig. 3.13 Data Acquisition (DR 230, YOKOGAWA)



Fig. 3.14 VA meter (Model : PW3198, HIOKI)

3.2.3 Experimental case

The experiment can be divided into an experiment to find the optimal condition of heat pipe operation and an experiment to measure the performance. The case of experiments to find the optimal case are summarized in Table 3.1. Selection of the refrigerant and the optimal filling rate were confirmed through the experiment. According to the Chapter 2, water is theoretically expected to be the optimal working fluid. The performance was compared experimentally with FC-72.

To decide the optimal filling rate, considering the filling rate of the conventional type, 1300 cc was determined as the smallest amount of working fluid among the experimental cases. The performance was measured by increasing the amount of working fluid from 1300 cc to 1700 cc. Heat pipe performance test was carried out based on the standard operating environment of 2400 W heat generation and driving wind speed of 3 m/s. In the end, the two optimal filling rates with excellent performance tests were conducted by the driving wind from 1m/s to 5m/s and the thermal load of 1800 W to 3600 W. Experiments were carried out on various cases as shown in Table 3.2, and finally, the working fluid and the working fluid filling rate were determined as the optimal operating condition.

After determining the optimal operating conditions for the

conventional type and the loop type, a performance comparison experiment was conducted as shown in Table 3.3. The performance comparison experiment is divided into ΔT (the difference between maximum temperature of IGBTs and the ambient temperature) measurement with the calculation of maximum cooling capacity and temperature uniformity measurement of IGBT module.

ΔT was measured for each heat pipe module while changing the thermal load from 1800 W to 4500 W at driving wind of 1 m/s, 3 m/s, and 5 m/s. The maximum value of ΔT required to maintain the performance of the IGBT module suggested by the railroad company is 60°C. Based on this, the maximum cooling capacity and thermal resistance for each case were calculated and compared.

The degree of temperature uniformity was compared for each case. The temperature distribution of IGBT for each case was expressed schematically. The uniformity was calculated by the standard deviation and the difference between the maximum and minimum temperature of each IGBT #1, #2, and #3.

Finally, a separate additional experiment was conducted to confirm the effect of the reservoir regarding the temperature uniformity.

Table 3.1 Experiment case of optimal operation condition (refrigerant)

| Working fluid | Quantity of working fluid | | | | | | |
|--------------------------|----------------------------------|---------------|---------------|---------------|---------------|---------------|---------------|
| | 1300cc | 1400cc | 1500cc | 1550cc | 1600cc | 1650cc | 1700cc |
| FC-72 | WF_F_1 | WF_F_2 | WF_F_3 | - | WF_F_5 | - | - |
| Water | WF_W_1 | WF_W_2 | - | WF_W_4 | WF_W_5 | WF_W_6 | WF_W_7 |

Table 3.2 Experiment case of optimal operation condition (quantity)

| Quantity of Refrigerant | Driving | Thermal Load | | | | | |
|-------------------------------|---------|--------------|---------|---------|---------|---------|---------|
| | Wind | 1800 W | 2400 W | 3000 W | 3600 W | 4200 W | 4500 W |
| 1600 CC | 1 m/s | QF1_1_1 | QF1_1_2 | QF1_1_3 | QF1_1_4 | - | - |
| | 3 m/s | QF1_3_1 | QF1_3_2 | QF1_3_3 | QF1_3_4 | - | - |
| | 5 m/s | - | - | QF1_5_3 | QF1_5_4 | - | - |
| 1650 CC | 1 m/s | QF2_1_1 | QF2_1_2 | QF2_1_3 | QF2_1_4 | - | - |
| | 3 m/s | QF2_3_1 | QF2_3_2 | QF2_3_3 | QF2_3_4 | - | - |
| | 5 m/s | - | - | QF2_5_3 | QF2_5_4 | QF2_5_5 | QF2_5_6 |

Table 3.3 Experiment case of performance analysis

| Type of Heat pipe | Driving | Thermal Load | | | | | |
|--|---------|--------------|---------|---------|---------|---------|---------|
| | Wind | 1800 W | 2400 W | 3000 W | 3600 W | 4200 W | 4500 W |
| Conventional Heat pipe (Type #1) | 1 m/s | HP1_1_1 | HP1_1_2 | HP1_1_3 | HP1_1_4 | - | - |
| | 3 m/s | HP1_3_1 | HP1_3_2 | HP1_3_3 | HP1_3_4 | - | - |
| | 5 m/s | - | - | HP1_5_3 | HP1_5_4 | HP1_5_5 | HP1_5_6 |
| Loop type Heat pipe (Type #2) | 1 m/s | HP2_1_1 | HP2_1_2 | HP2_1_3 | HP2_1_4 | - | - |
| | 3 m/s | HP2_3_1 | HP2_3_2 | HP2_3_3 | HP2_3_4 | - | - |
| | 5 m/s | - | - | HP2_5_3 | HP2_5_4 | HP2_5_5 | HP2_5_6 |

Chapter 4. Experimental results

4.1 Optimal working conditions

Through the experiment, the refrigerant and the optimal refrigerant filling rate were determined.

4.1.1 Determining refrigerant

Theoretically, the optimal working fluid is expected to be water in this study, but for experimental confirmation, the performance was compared by experiments when the working fluid was water and FC-72. For accurate performance comparison regardless of the optimal amount of working fluid, the experiment was conducted while increasing the amount of working fluid from 1300 cc to 1700 cc. The experiment was carried out in the case of a driving wind of 3 m/s and a thermal load of 2400 W, which is the standard case.

In the case of FC-72, when the working fluid amount was 1300 cc and 1400 cc, the heat pipe could not operate due to overheating with dry-out. In these cases, the increase of the temperature did not stop even when ΔT reached about 100 K, so the experiment was stopped in the middle. In the case of working fluid volume of 1500 cc and 1600

cc, the heat pipe operated normally, but the ΔT was 71.5 K and 70.5 K respectively which exceeded the target ΔT of 60 K, and failed to achieve the target performance. The change of ΔT by the time for each working fluid amount is shown in Figure 4.1.

In the case of using water as the refrigerant in the same way, the target was achieved for the ΔT to be less than 60 K. As in the case of using FC-72, when the amount of working fluid was 1300 cc, the heat pipe did not work normally due to overheating with dry-out. When the amount of working fluid is 1400 cc, the temperature converges, but ΔT is 86.9 K, failing to achieve the target performance. When the amount of working fluid was 1550 cc, ΔT was lower than 60 K and the target performance was achieved. The ΔT change by the time and the amount is shown in Figure 4.2.

The experimental results when FC-72 and water were used as working fluids are summarized in Table 4.4. Based on the results and a related theory in Chapter 2, water was determined as the refrigerant.

4.1.2 Optimal filling rate of refrigerant

The performance varies depending on the amount of refrigerant, so it is important to study the optimal amount of refrigerant. To determine the optimal filling rate of the loop type, an experiment was conducted by increasing the amount of water from 1300 cc to 1700 cc. The experimental results in case of forced convection of 3 m/s and thermal load of 2400 W are shown in Figure 4.3. When the working fluids were 1300 cc and 1400 cc, overheating due to dry-out occurred and normal operation was impossible. In case of 1550 cc, the performance ΔT was 53 K, less than the target ΔT of 60 K and the target performance was achieved. According to the results of experiment, in case of 3 m/s driving wind and 2400 W thermal load, the optimal amount of working fluid for loop type was 1650 cc with the ΔT of 42.7 K, the minimum ΔT among the all cases. When the amount of working fluid was 1600 cc and 1700 cc, ΔT was 48.5 K and 47.9 K, respectively, higher than 42.7 K.

The optimal working fluid filling rate of the loop type heat pipe was around 34.4% in the case of the amount of refrigerant 1650 cc. This value is higher than the optimal filling rate of the conventional type of around 15%. The reason why the optimal filling rate of the loop type is higher than that of the conventional heat pipe is due to the

difference in inside volume. In the case of a loop type, unlike a conventional type, reservoirs and a return pipe exist separately. Since the reservoir under the evaporator should be filled with working fluid for the stable operation, it is analyzed that more working fluid is required.

In order to confirm the 1650 cc as an optimal amount of refrigerant for the manufactured loop type, the experiments in Table 4.2 were conducted, respectively, and the results are shown in Figure 4.4 and Table 4.5. Performance of 1650 cc was better in all the cases conducted, and it was experimentally confirmed that 1650 cc and the filling rate of 34.4% were the optimal operation conditions regarding the working fluid.

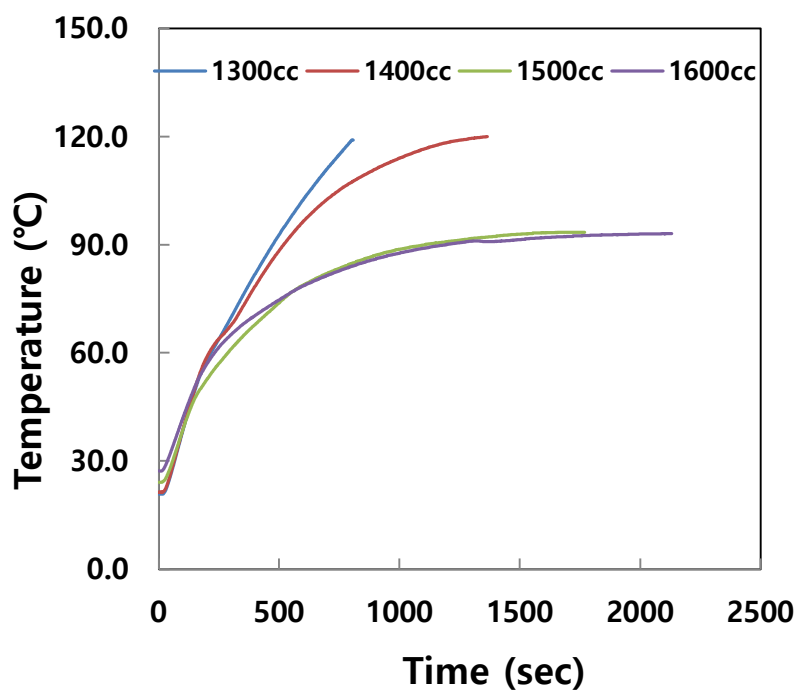


Fig. 4.1 ΔT by the quantity of working fluid (FC-72)

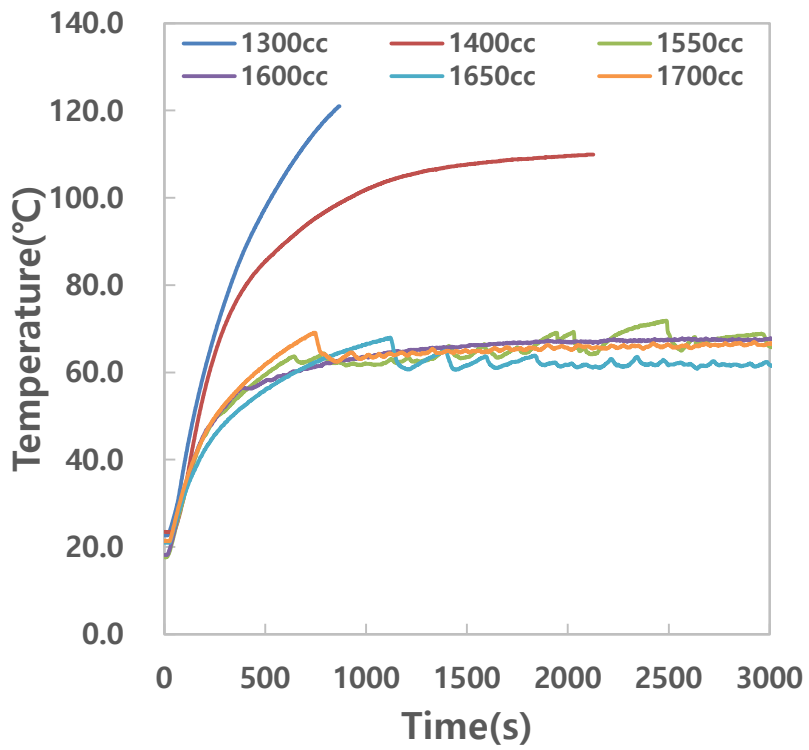


Fig. 4.2 Temperature by the quantity of working fluid (Water)

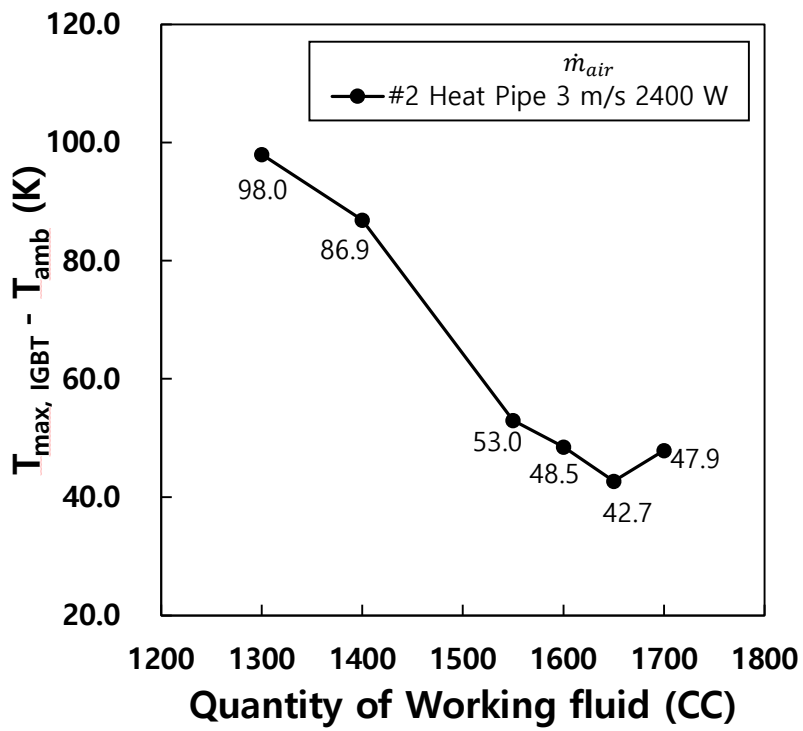


Fig. 4.3 ΔT by the quantity of working fluid (water)

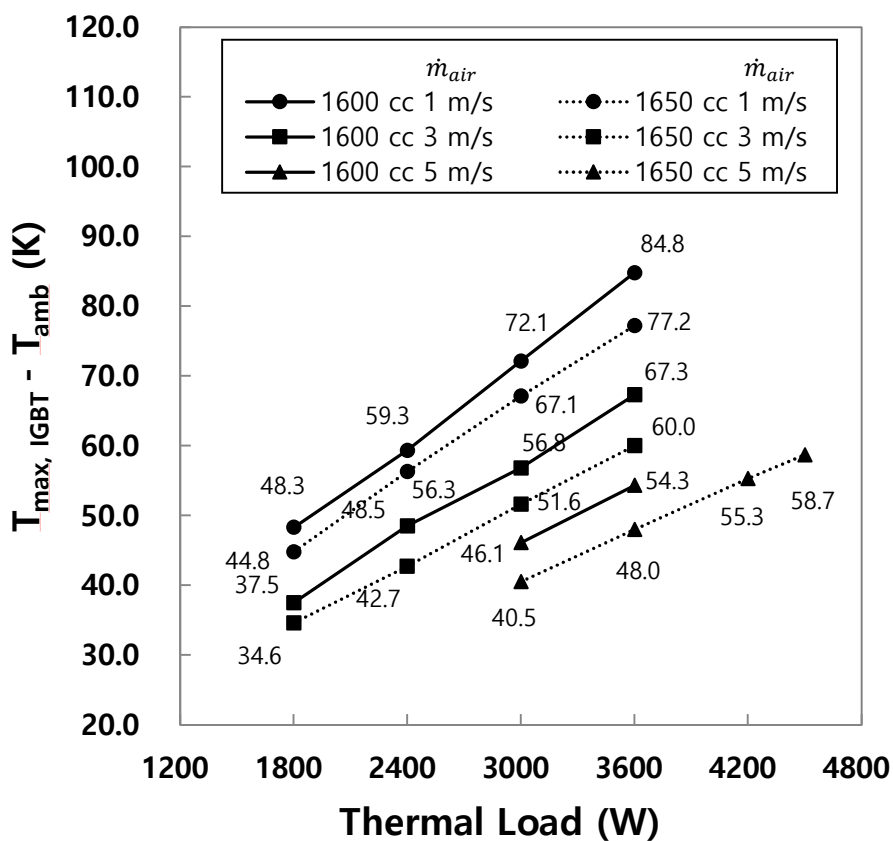


Fig. 4.4 Performance comparison of 1600 cc and 1650 cc

Table 4.1 ΔT by the working fluid

| Working fluid | Quantity of working fluid | | | | | | |
|--------------------------|----------------------------------|---------------|---------------|---------------|---------------|---------------|---------------|
| | 1300cc | 1400cc | 1500cc | 1550cc | 1600cc | 1650cc | 1700cc |
| FC-72 | 97.8 K | 98.0 K | 71.1 K | - | 70.5 K | - | - |
| Water | 98.0 K | 86.9 K | - | 53.0 K | 48.5 K | 42.7 K | 47.9 K |

Table 4.2 ΔT by the quantity of working fluid

| Quantity of Refrigerant | Driving Wind | Thermal Load | | | | | |
|-------------------------------|-----------------|--------------|--------|--------|--------|--------|--------|
| | | 1800 W | 2400 W | 3000 W | 3600 W | 4200 W | 4500 W |
| 1600 CC | 1 m/s | 48.3 K | 59.3 K | 72.1 K | 84.8 K | - | - |
| | 3 m/s | 37.5 K | 48.5 K | 56.8 K | 67.3 K | - | - |
| | 5 m/s | - | - | 46.1 K | 54.3 K | - | - |
| 1650 CC | 1 m/s | 44.8 K | 56.3 K | 67.1 K | 77.2 K | - | - |
| | 3 m/s | 34.6 K | 42.7 K | 51.6 K | 60.0 K | - | - |
| | 5 m/s | - | - | 40.5 K | 48.0 K | 55.3 K | 58.7 K |

4.2 Results of performance

The performance in this study is ΔT ($\Delta T_{max,IGBT} - \Delta T_{amb}$) and temperature uniformity. In this study, for the reliable use of IGBT module, ΔT should be maintained below 60 K for the heat pipe to be applied to the train. There is no standard for temperature uniformity, but the more uniform distribution of heat the better.

4.2.1 Maximum cooling capacity

An experiment was conducted to measure the cooling performance of conventional type and loop type one by reflecting the optimal operating conditions.

4.2.1.1 Performance of the conventional type

The measured IGBT temperature by the time of the conventional type at base case, 3 m/s driving wind and 2400 W thermal load, is shown in Figure 4.5. The ΔT was 46.3 K and the target performance was achieved. Although there was a temperature difference between the three IGBTs, the temperatures all converge.

To calculate the maximum cooling capacity of the heat pipe, ΔT was

measured in the case of the thermal load from 1800 W to 4500 W. ΔT by the time for each thermal load in 3 m/s forced convection can be seen in Figure 4.7. Even when the thermal load is 3600 W, the temperature converges and cooling is performed, but ΔT is 67.6 K, which makes it fail to achieve the target performance. But, when the thermal load was 3000 W, ΔT reached 56.6 K. If the maximum cooling capacity is calculated using linear interpolation based on the ΔT of each case, the maximum cooling capacity of the conventional heat pipe at 3m/s forced convection is calculated as 3185 W.

The experiment was conducted in the same way when the forced convection was 1 m/s and 5 m/s. The results are expressed in Figure 4.6 and Figure 4.8, respectively. In all cases, the ΔT values reached a converging steady state, but in some cases, the ΔT exceeded 60K and the target performance was not reached. In the case of forced convection 1 m/s, the target performance was achieved with a ΔT value of 59.6 K up to a thermal load of 2400 W. In the case of forced convection of 5 m/s, the value of ΔT was about 60 K up to a thermal load of 4500 W, resulting in the target performance level. The ΔT for all the cases conducted is shown in Figure 4.9.

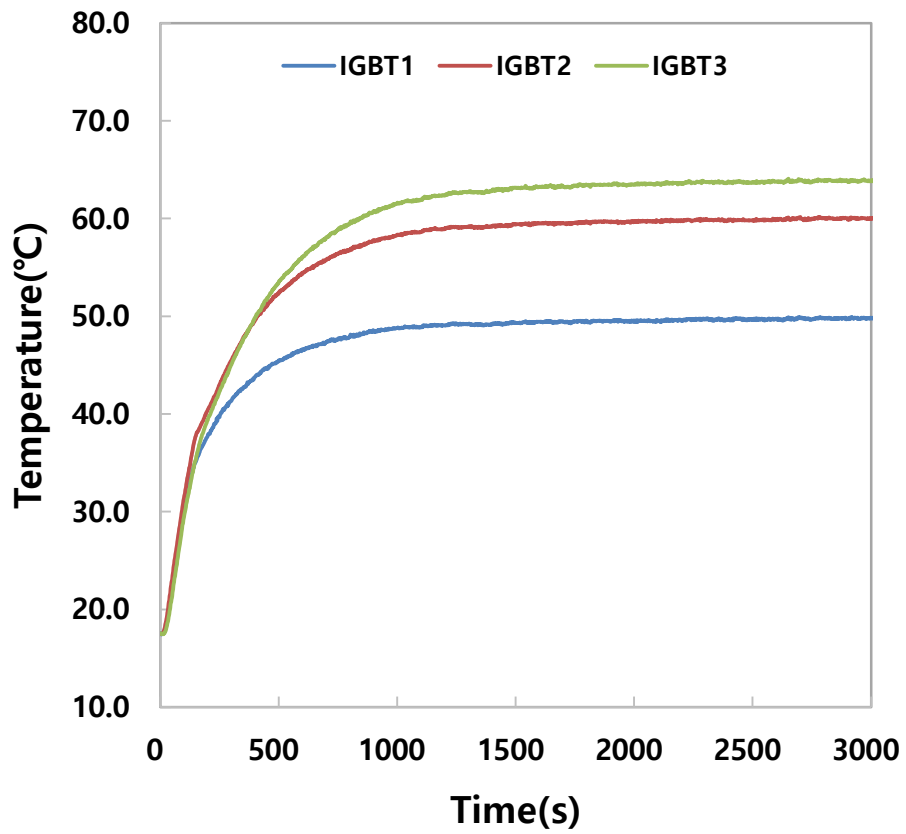


Fig. 4.5 IGBT temperature of conventional heat pipe
(3 m/s, 2400 W)

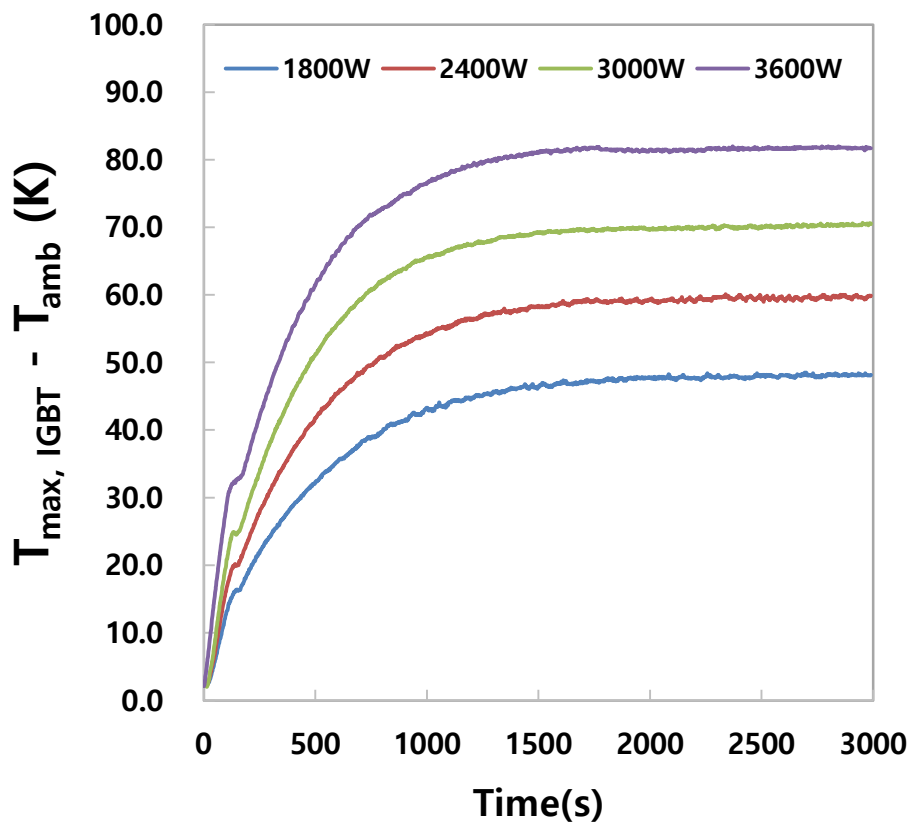


Fig. 4.6 Conventional type ΔT
(1 m/s forced convection)

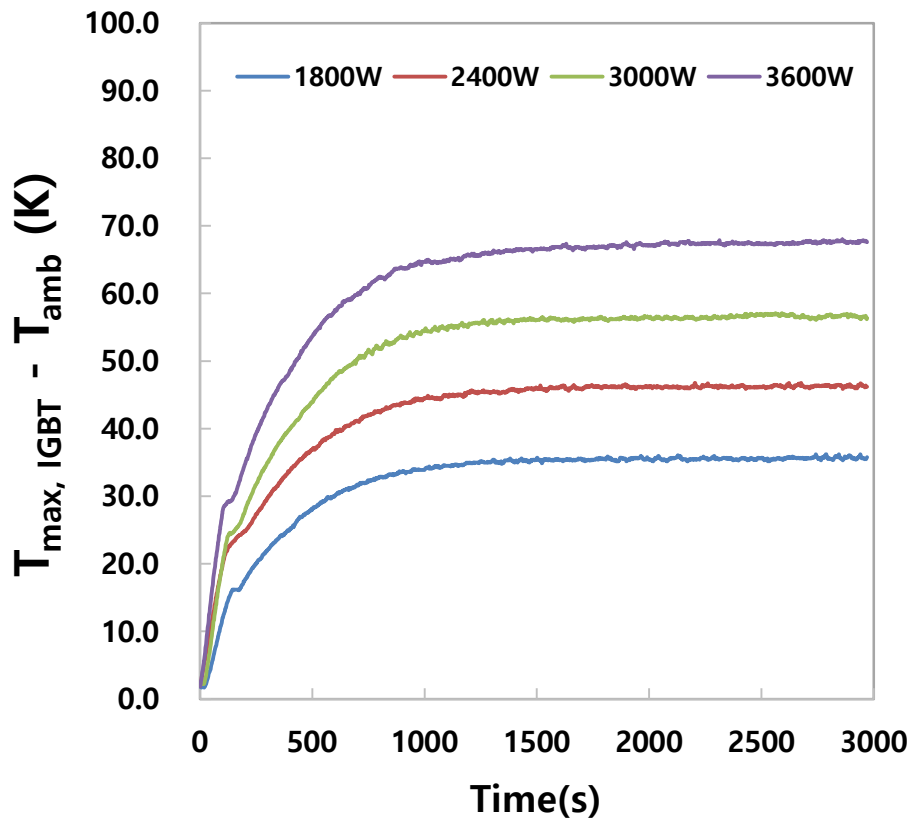


Fig. 4.7 Conventional type ΔT
(3 m/s forced convection)

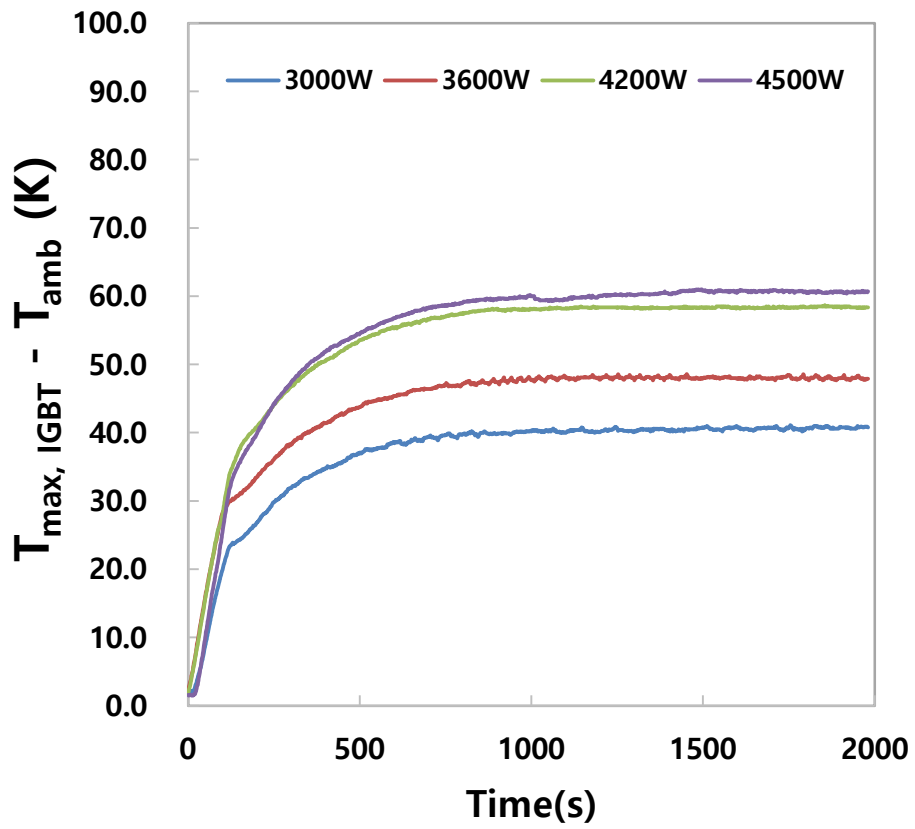


Fig. 4.8 Conventional type ΔT
(5 m/s forced convection)

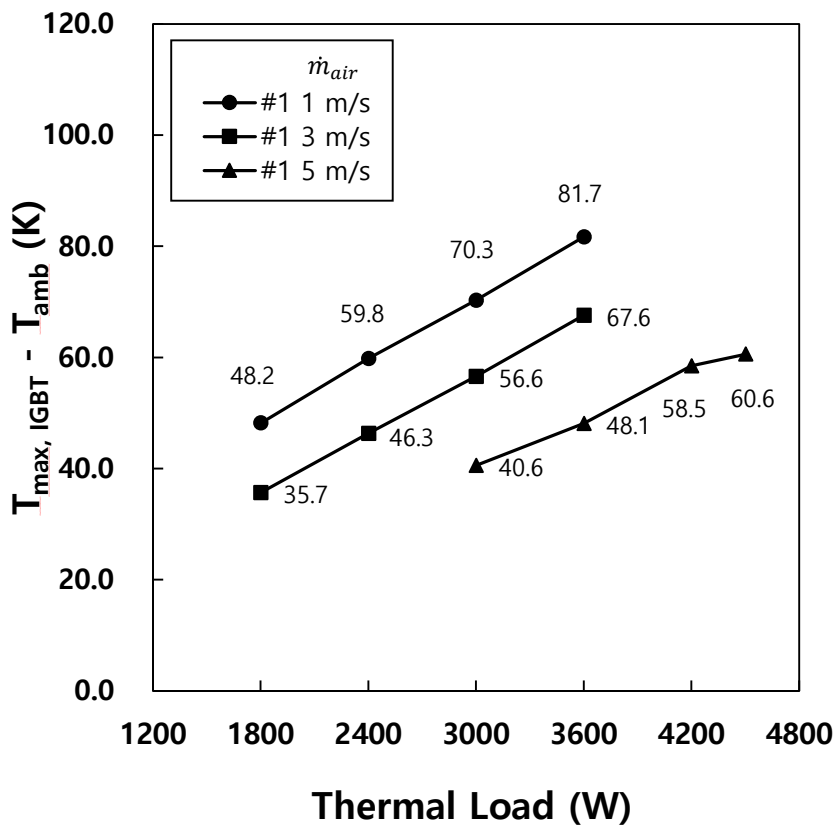


Fig. 4.9 Performance of conventional heat pipe (Type #1)

4.2.1.2 Performance of the loop type heat pipe

The same method of experiment was conducted for the loop type. Temperature by the time of the loop type at base case, 3 m/s driving wind and 2400 W thermal load, is shown in Figure 4.10. ΔT was measured as 42.7 K, achieving target performance, and it was 3.6 K lower than the conventional heat pipe. Although the degree of temperature fluctuate from initial start-up to stabilization state is greater than that of conventional heat pipes, it is at a level that is not a problem when applied to IGBT module cooling. The ΔT by the time for each thermal load in 3 m/s forced convection can be seen in Figure 4.12. Even when the thermal load is 3600 W, the temperature converges and ΔT is 60 K, achieving the target performance. At 3 m/s forced convection, the maximum cooling capacity of the loop type is 3600 W. Experiment was conducted in the same way when the forced convection was 1 m/s and 5 m/s, respectively. The results are expressed in Figure 4.11 and Figure 4.13.

In all cases, the ΔT reached a converging steady state, but in some cases, the ΔT exceeded 60 K and the target performance was not reached. The target performance was not achieved only when the thermal load was 3000 W or more in forced convection of 1 m/s among the cases in which the experiment was conducted. In the case of

forced convection 1 m/s, the target performance was achieved with a ΔT of 59.6 K up to a thermal load of 2400 W. For forced convection of 5m/s, the target performance was achieved with a value of ΔT of 58.7 K even at a thermal load of 4500 W. The ΔT for all the cases conducted is shown in Figure 4.14.

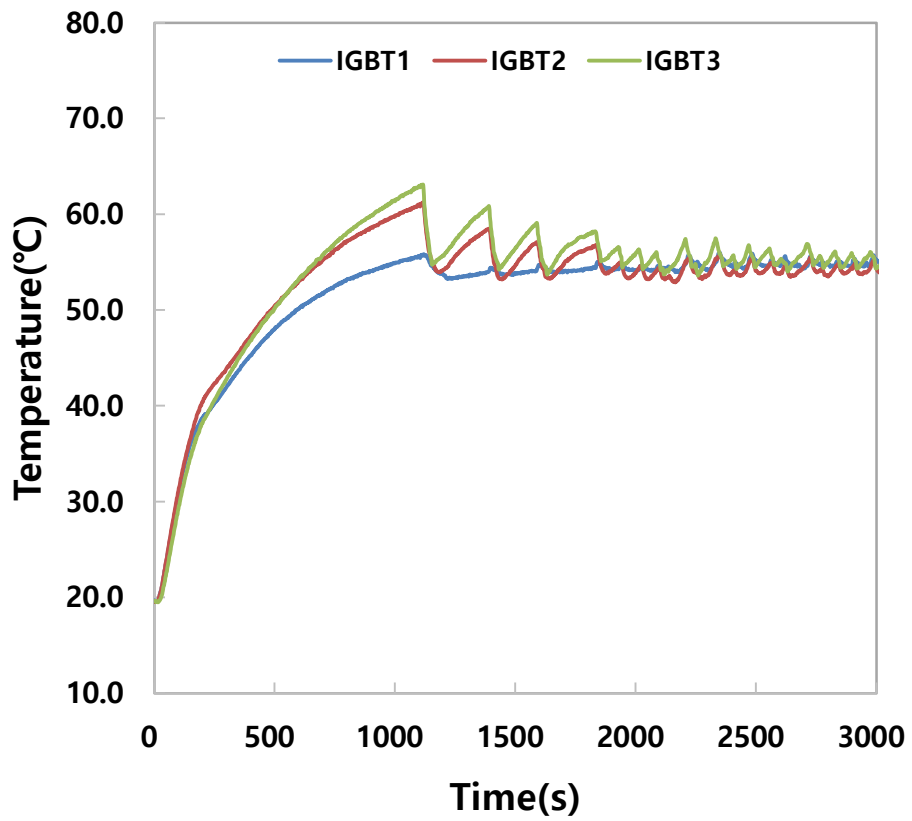


Fig. 4.10 IGBTs temperature of loop type heat pipe
(3 m/s, 2400 W)

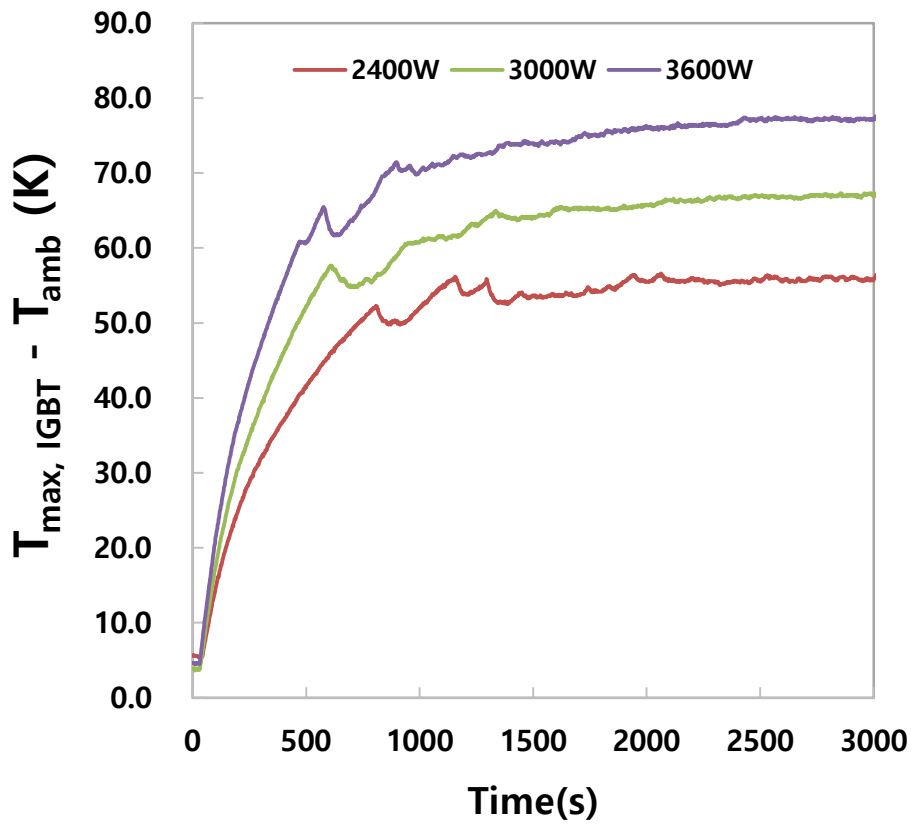


Fig. 4.11 Loop type heat pipe ΔT
(1 m/s forced convection)

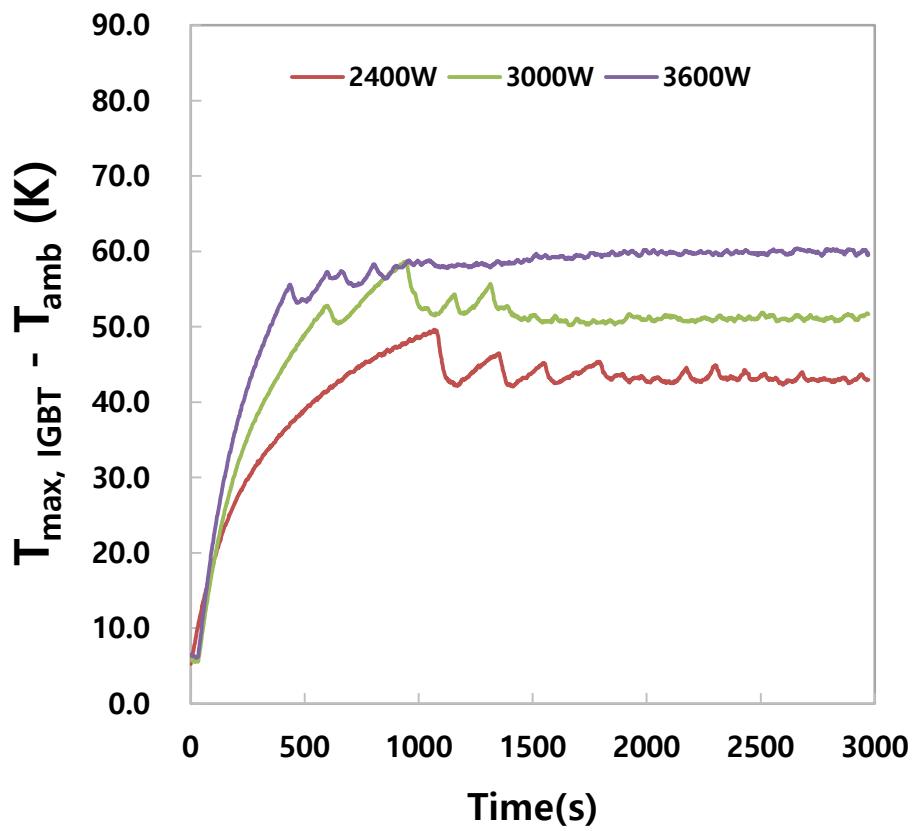


Fig. 4.12 Loop type heat pipe ΔT
(3 m/s forced convection)

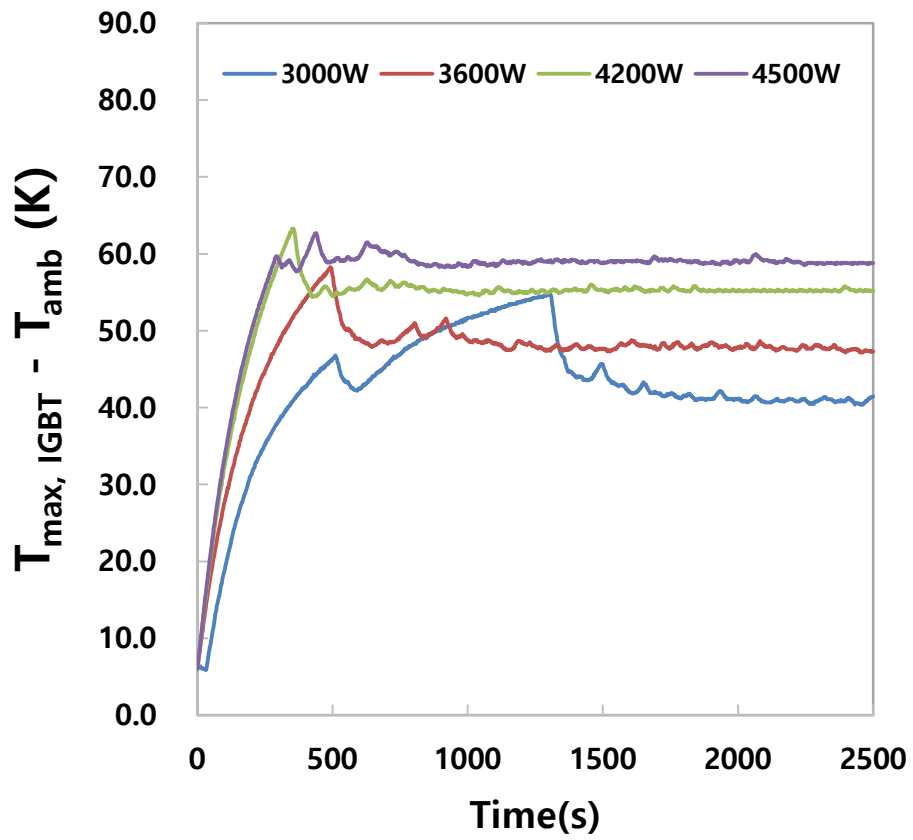


Fig. 4.13 Loop type heat pipe ΔT
(5 m/s forced convection)

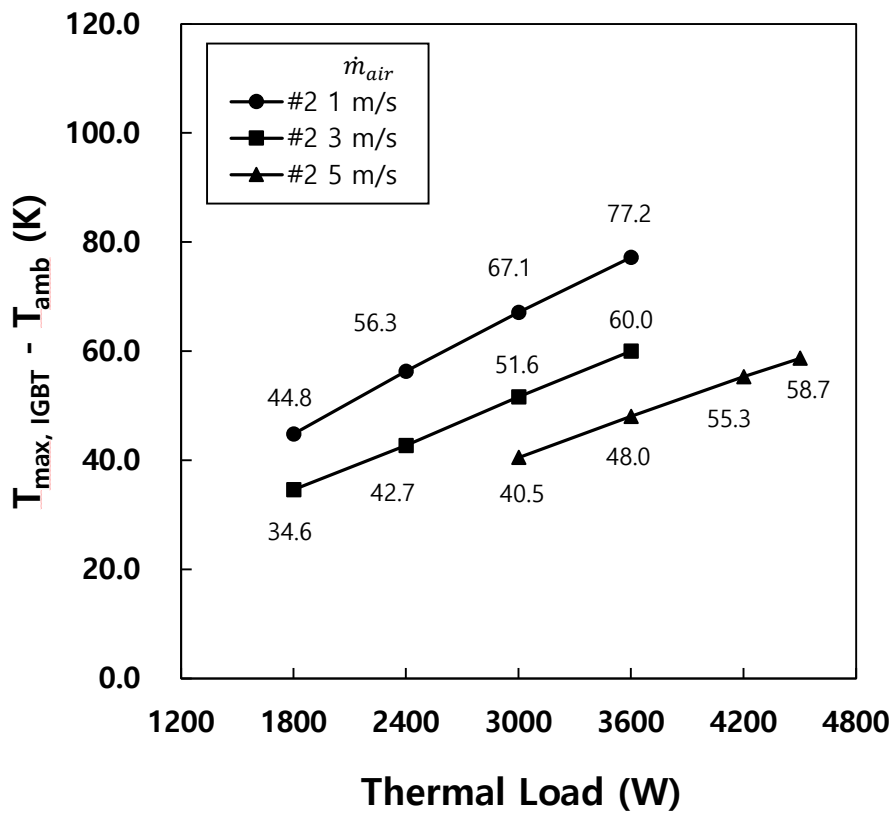


Fig. 4.14 Performance of loop type (Type #2)

The ΔT of the loop type changes slightly with time even if it converges. The change is about 1.0 K level, so there is no problem in using the IGBT module.

Figure 4.15 shows the comparison of ΔT of conventional type and loop type. On average, the ΔT of the loop type was 5.2% lower than that of the conventional type, showing better performance.

The thermal load with a ΔT of 60 K was the maximum cooling capacity for each case, and it was estimated and calculated using linear interpolation. In the base case, the maximum cooling capacity of the conventional type and the loop type was 3185 W and 3600 W, respectively, and the loop type heat pipe had about 8.1% higher cooling capacity. Accordingly, the resistances of the cooling system were 0.019°C/W and 0.018°C/W, respectively, and the resistance of the loop type was about 5.5% lower than that of the conventional type.

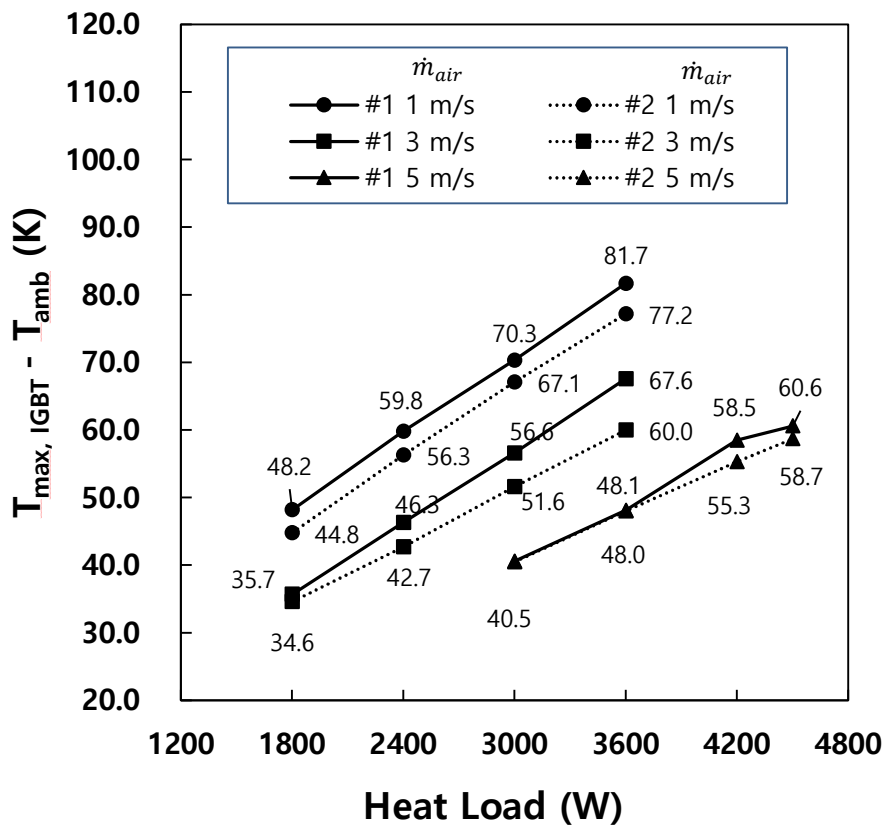


Fig. 4.15 Performance comparison of heat pipe #1 and #2

Table 4.3 Experiment results of performance

| Type of Heat pipe | Driving | Thermal Load | | | | | |
|--|---------|--------------|--------|--------|--------|--------|--------|
| | Wind | 1800 W | 2400 W | 3000 W | 3600 W | 4200 W | 4500 W |
| Conventional Heat pipe (Type #1) | 1 m/s | 48.2 K | 59.8 K | 70.3 K | 81.7 K | - | - |
| | 3 m/s | 35.7 K | 46.3 K | 56.6 K | 67.6 K | - | - |
| | 5 m/s | - | - | 40.5 K | 48.1 K | 58.5 K | 60.6K |
| Loop type Heat pipe (Type #2) | 1 m/s | 44.8 K | 56.3 K | 67.1 K | 77.2 K | - | - |
| | 3 m/s | 34.6 K | 42.7 K | 51.6 K | 60.0 K | - | - |
| | 5 m/s | - | - | 40.5 K | 48.0 K | 55.3 K | 58.7 K |

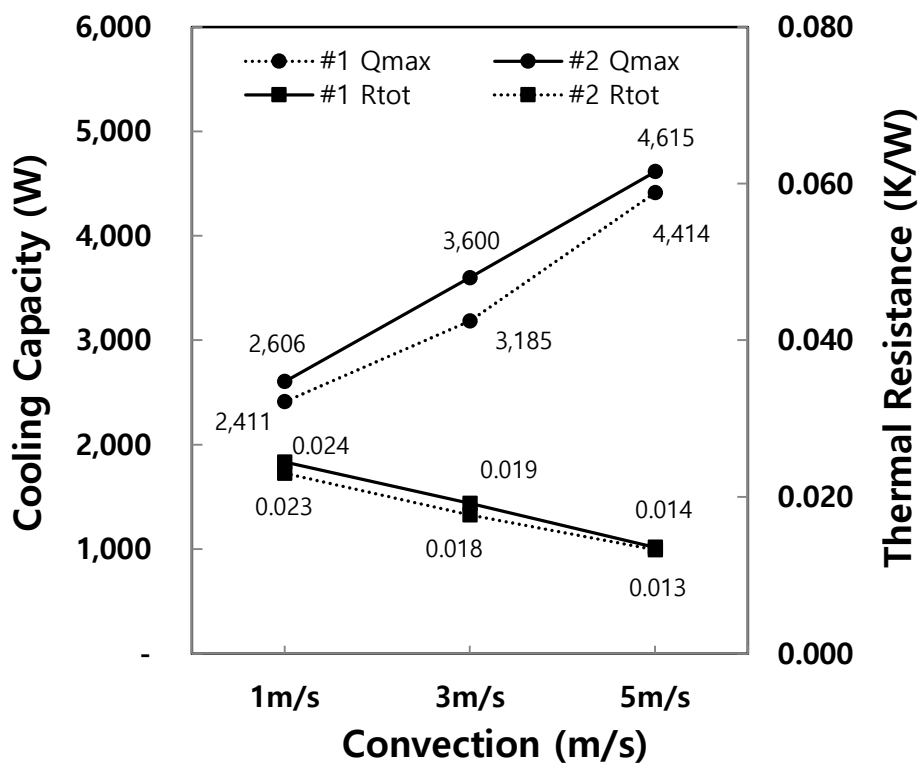


Fig. 4.16 Maximum cooling capacity of heat pipe #1 and #2

4.2.2 Temperature uniformity

The temperature uniformity of heat pipe is important performances by the applied application. In an IGBT module, the uniformity of temperature can affect the IGBT lifetime.

Fig. 4.17 shows the measured temperature of each IGBTs when a conventional type is installed in an environment of 3 m/s driving wind and 2400 W heat supply. There was a large average temperature difference of about 14 K between IGBT1 and IGBT3. This is due to the installation environment in which the influence of the driving wind for each IGBT cannot be the same. IGBT1, which is located close to the wind tunnel, was affected by the driving wind more than IGBT3, so the average temperature of IGBT1 was measured to be lower than that of IGBT3. The maximum temperature difference among the 9 temperature measurement points was 16.6 K, and the standard deviation of the measurement temperatures was calculated as 6.4.

Figure 4.18 indicates the temperature of each IGBTs in the case of a loop type system with 3 m/s forced convection and 2400 W thermal load. The average temperature was measured similarly for all IGBTs. The average temperature difference between IGBTs was 1.0 K, and the temperature uniformity was superior to than that of a conventional type. The maximum temperature differences among the 9 measured

points were 14.5 K, and the standard deviation of the measured temperature was 5.0. This is superior to the conventional heat pipe calculated by 16.6 K and 6.4, respectively.

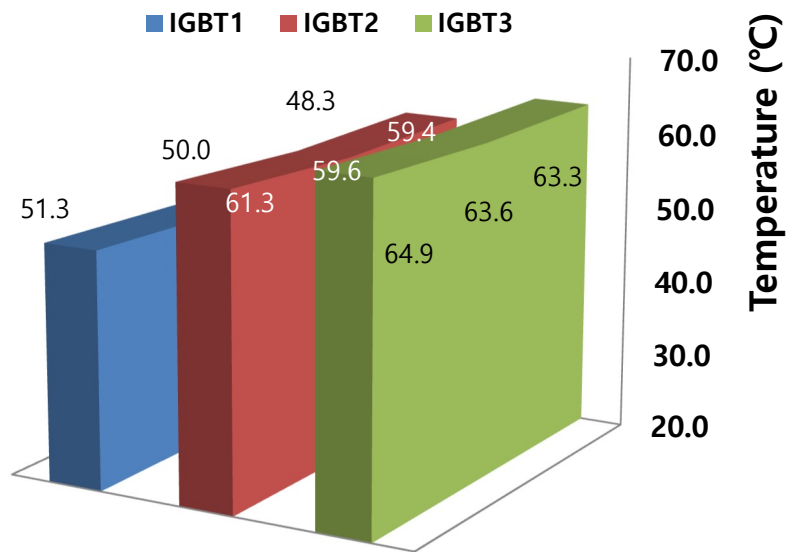


Fig. 4.17 Temperature of each IGBT in conventional heat pipe

Table. 4.4 Temperature of each IGBT in conventional heat pipe

| IGBT1 | | IGBT2 | | IGBT3 | |
|---------|---------------------|---------|---------------------|---------|---------------------|
| Spot | Temperature (°C) | Spot | Temperature (°C) | Spot | Temperature (°C) |
| #7 | 48.3 | #8 | 59.4 | #9 | 63.3 |
| #4 | 50.0 | #5 | 59.6 | #6 | 63.6 |
| #1 | 51.3 | #2 | 61.3 | #3 | 64.9 |
| Average | 49.9 | Average | 60.1 | Average | 63.9 |

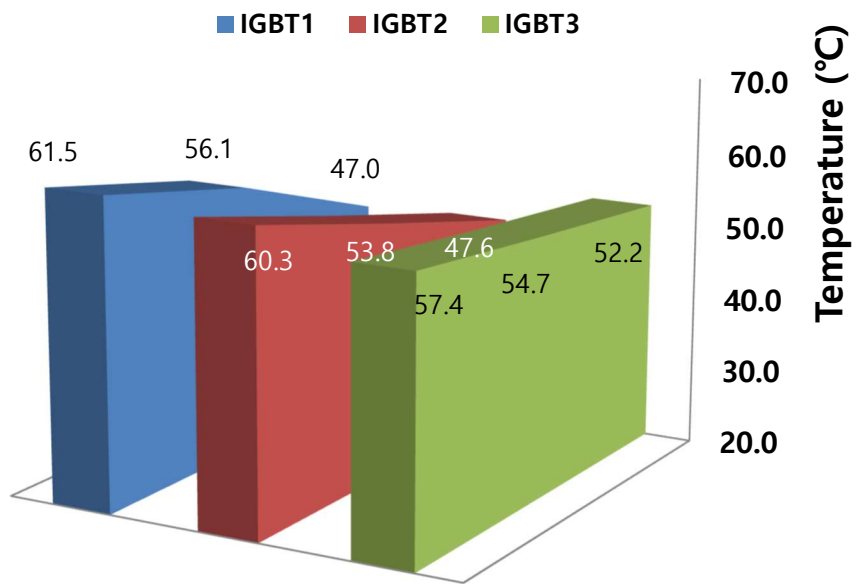


Fig. 4.18 Temperature of each IGBT in loop type heat pipe

Table. 4.5 Temperature of each IGBT in loop type heat pipe

| IGBT1 | | IGBT2 | | IGBT3 | |
|---------|---------------------|---------|---------------------|---------|---------------------|
| Spot | Temperature (°C) | Spot | Temperature (°C) | Spot | Temperature (°C) |
| #7 | 47.0 | #8 | 47.6 | #9 | 52.2 |
| #4 | 56.1 | #5 | 53.8 | #6 | 54.7 |
| #1 | 61.5 | #2 | 60.3 | #3 | 57.4 |
| Average | 54.9 | Average | 53.9 | Average | 54.8 |

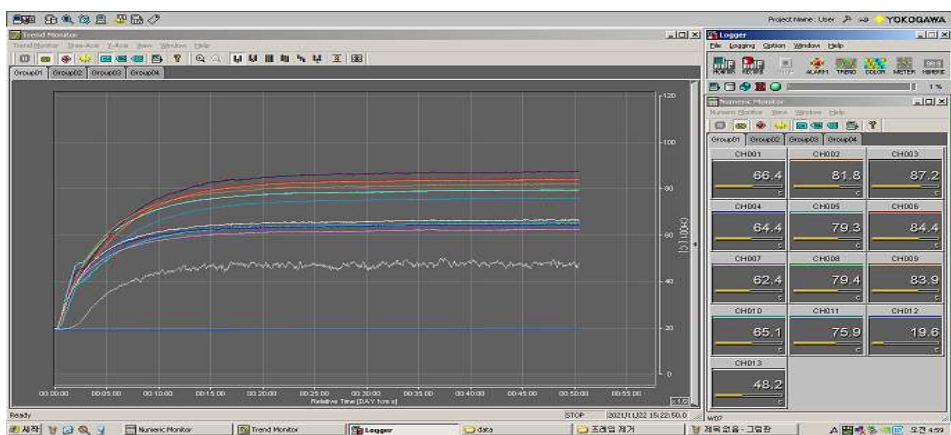


Fig. 4.19 Temperature of Type #1 (3 m/s, 3600 W)

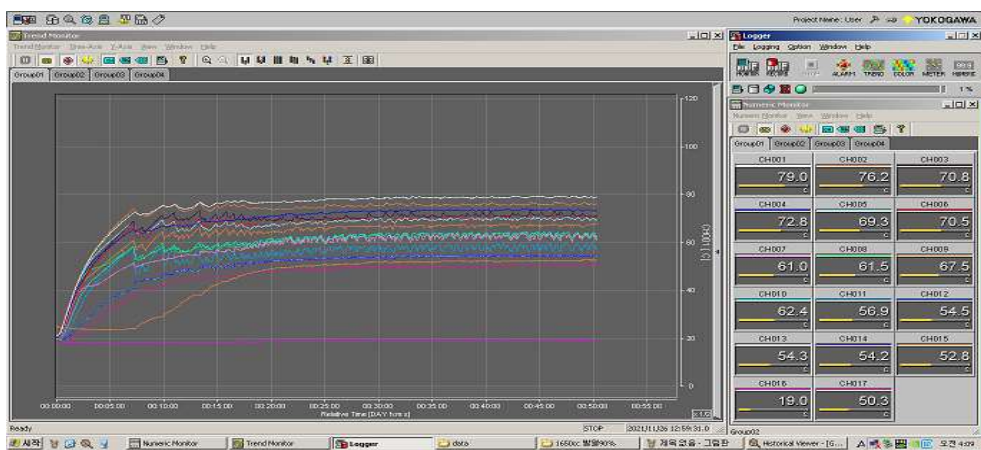


Fig. 4.20 Temperature of Type #2 (3 m/s, 3600 W)

The standard deviation and temperature differences of conventional type and loop type depending on the thermal load are shown in Figure 4.11. The temperature uniformity was better in loop type as the thermal load increased. For each heat pipe, when the forced convection was 3 m/s and the thermal load was 3600 W, the temperature change with time is expressed in Figure 4.19 and Figure 4.20. When the temperature converges, the temperature deviation of the loop type is smaller than that of the conventional type. However, there was a temperature deviation within the IGBT in the case of loop type, which seems to be the effect of heat conduction of the refrigerant stored in the manifold reservoir. This part is expected to be improved by minimizing the size of the reservoir.

To find out whether the temperature deviation in the IGBT of the loop type is the effect of the reservoir, a new type as shown in Figure 2.11 was manufactured. This is a heat pipe in which only the reservoir under the evaporator is installed in the conventional type, and the rest parts is the same. Results of experiment in the base case are shown in Figure 4.22 and Figure 4.23. According to the Table 4.6 and Table 4.7, the temperature deviation in the IGBT module increased from 2.0 K to 6.2 K as the installation of reservoir. As a result of this additional experiment, it is confirmed that the relatively large temperature deviation in the IGBT in the loop type is due to the influence of the

reservoir. Therefore, it was found that minimizing the volume of the manifold for connecting each heat pipes is better for performance when manufacturing loop type heat pipes.

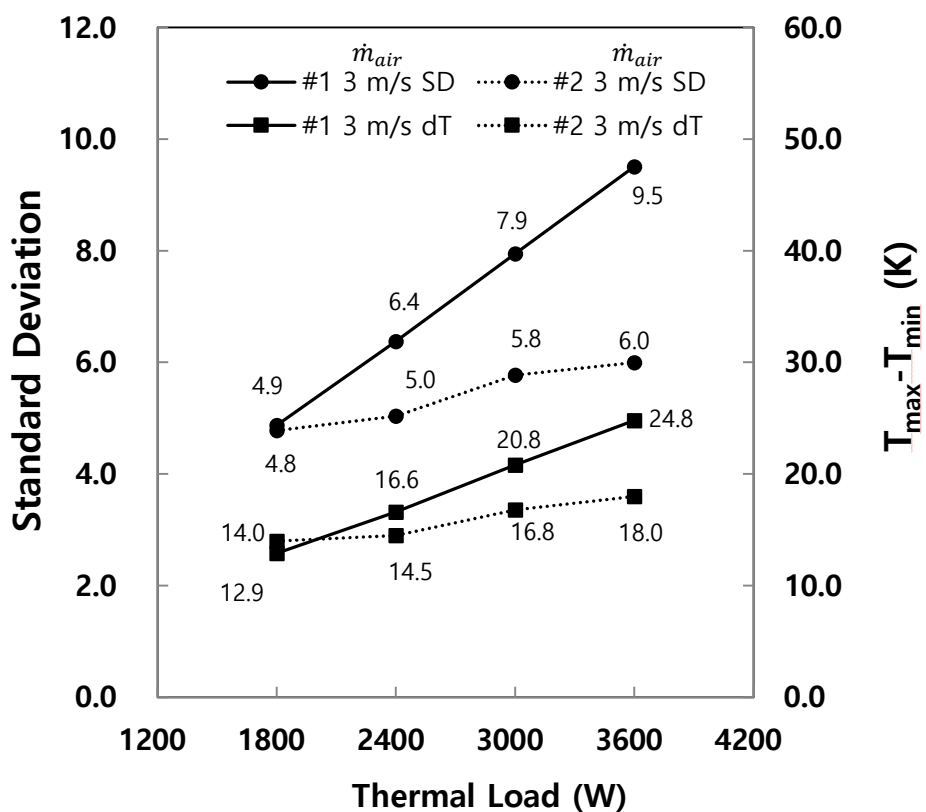


Fig. 4.21 Comparison of heat distribution

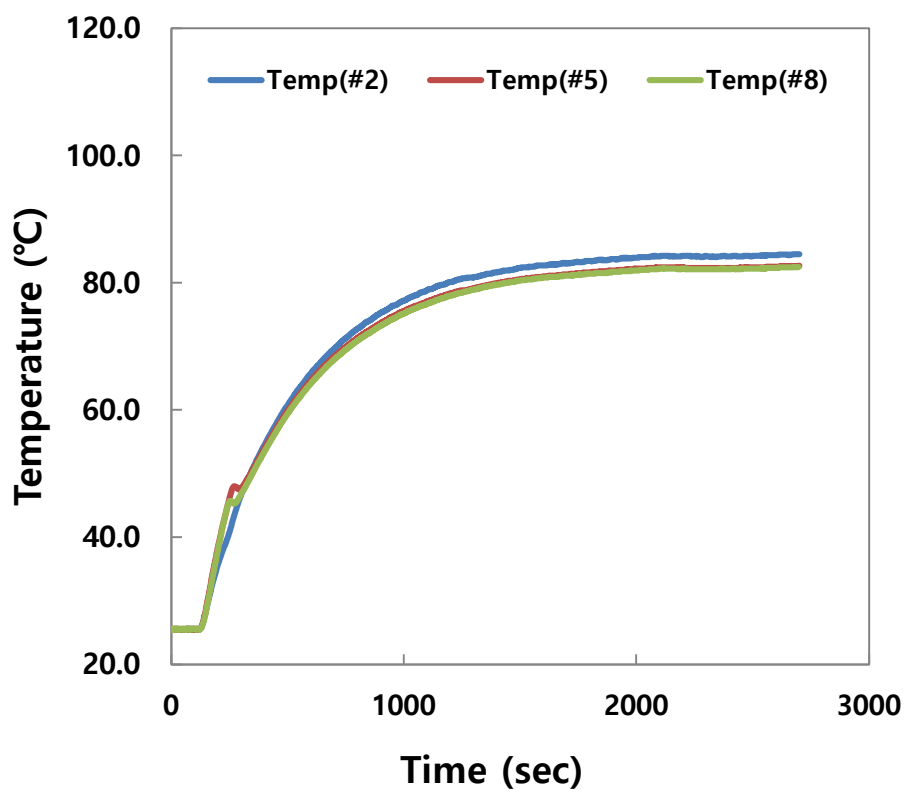


Fig. 4.22 Performance of Type #2

Table 4.6 IGBT Temperature of Heat Pipe Type #2

| IGBT1 | | IGBT2 | | IGBT3 | |
|-------------------|---------------------|-------------------|---------------------|-------------------|---------------------|
| Spot | Temperature (°C) | Spot | Temperature (°C) | Spot | Temperature (°C) |
| #7 | 77.5 | #8 | 82.5 | #9 | 78.7 |
| #4 | 77.7 | #5 | 82.7 | #6 | 79.1 |
| #1 | 80.3 | #2 | 84.5 | #3 | 80.1 |
| T (#1)- T (#7) | 2.8 | T (#2)- T (#8) | 2.0 | T (#3)- T (#9) | 1.4 |

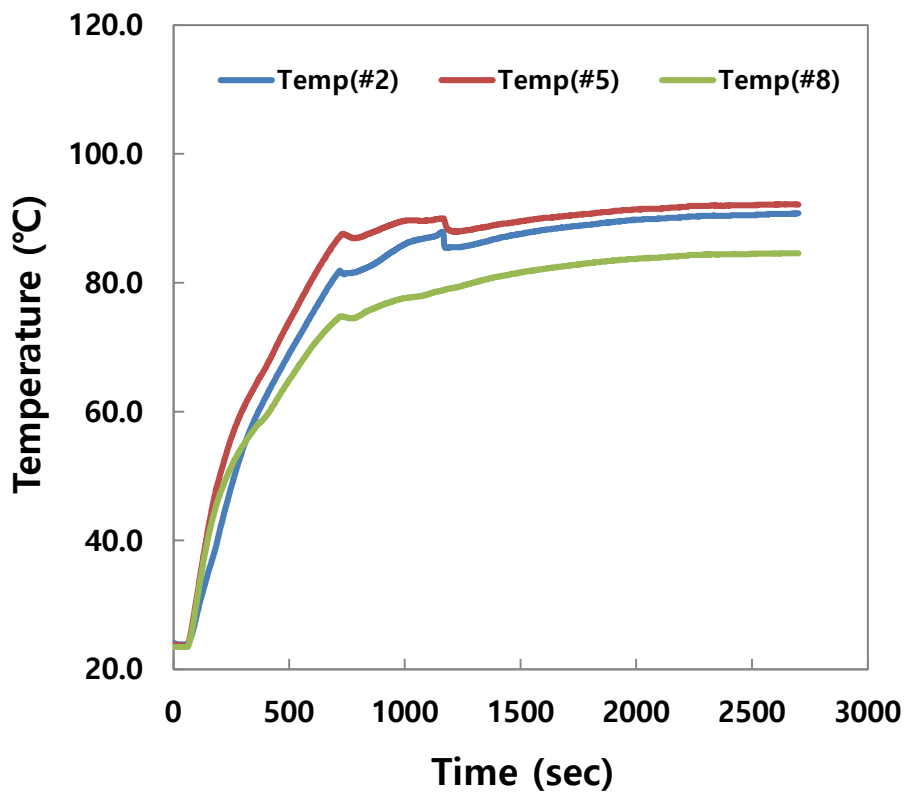


Fig. 4.23 Performance of Type #3

Table 4.7 IGBT Temperature of Heat Pipe Type #3

| IGBT1 | | IGBT2 | | IGBT3 | |
|-------------------|------------------|-------------------|------------------|-------------------|------------------|
| Spot | Temperature (°C) | Spot | Temperature (°C) | Spot | Temperature (°C) |
| #7 | 76.3 | #8 | 85 | #9 | 77.7 |
| #4 | 77.7 | #5 | 92.6 | #6 | 87.2 |
| #1 | 82.7 | #2 | 91.2 | #3 | 86.9 |
| T (#1)- T (#7) | 6.4 | T (#2)- T (#8) | 6.2 | T (#3)- T (#9) | 9.2 |

4.3 Discussion

Through the experiment, it was confirmed that the performance of the loop type was superior to that of the conventional type in terms of cooling capacity and heat uniformity.

In the case of a loop type, when the temperature converges, there is oscillation in the temperature, but the degree of oscillation is at around 1.0 K, and the effect on the IGBT module is insignificant. The time it takes for the temperature to converge from start-up is long compared to the conventional type, but the difference is not large, and it is not a problem due to the continuous operation tendency of the train. However, in terms of cooling capacity per unit capacity and cooling uniformity, a loop type is better.

The reason that the performance of the loop type is superior to that of the conventional type is that the resistance generated when the fluid circulates the heat pipe is smaller. Loop type has a separate return pipe where the fluid liquefied from the condenser returns, so the resistance with the refrigerant in the steam state that is relatively small. In a conventional type, the circulation of the liquid refrigerant liquefied in the condenser and the vaporized refrigerant in the evaporator occurs in one pipe, resulting in resistance, which leads to the entrainment limit discussed in Chapter 2.

According to Kim et. al [32], the flow friction coefficient of the entire system can be expressed as equation (4.1) below.

$$\sum_{i=1}^n F_i = F_{v,gr} + F_{v,l} + F_{l,l} + F_c + F_{sc} + F_{cc} + F_w \quad (4.1)$$

The maximum heat transfer limit is calculated by equation (4.2). [32]

$$(QL)_{c,max} = \frac{\Delta P}{(F_{v,gr} + F_{v,l} + F_{l,l} + F_c + F_{sc} + F_{cc} + F_w)} \quad (4.2)$$

Therefore, as the flow friction coefficient decrease, the maximum heat transfer amount increases. In Equation (4.1), the difference between the loop type and the conventional type is the friction coefficients F_v and F_l in the vapor and liquid transport pipes. Expressing each as an equation, it is (4.3) and (4.4). [32]

$$F_{v,l} = \left(\frac{1}{2}\right) \frac{(F_v Re_v) \mu_v}{d_v^2 A_v \rho_v \dot{h}_{lv}} \quad (4.3)$$

$$F_{l,l} = \left(\frac{1}{2}\right) \frac{(F_l Re_l) \mu_l}{d_l^2 A_l \rho_l \dot{h}_{lv}} \quad (4.4)$$

In equations (4.3) and (4.4), the variable related to the shape of the heat pipe is the diameter d. Each flow friction decreases as the

diameter increases. Although the size of the pipe used to manufacture the loop type and the conventional type is the same, the cross-sectional area of the vapor and liquid transport pipe is larger due to the return pipe in the loop type case. Therefore, it can be seen that the friction coefficient of the loop type is smaller, and the heat transfer amount is increased.

5. Conclusion

In this study, a conventional type (Type #1) and a loop type (Type #2) were applied for IGBTs for high-speed trains and subways. A loop heat pipe was manufactured by modifying the conventional heat pipe applied to the IGBT module of subway, and the optimal operating conditions were experimentally investigated. In addition, the cooling performance and cooling uniformity were calculated and measured, respectively, and compared by changing the driving wind and heat load conditions.

Figure of Merit of loop type is different from that of conventional heat pipe, but the performance of the water was the best, and the optimal filling rate was 34.4%, which was higher than that of the conventional pipe by around 15%. This difference occurred due to the volume of the reservoir added when designing the loop type system. In order to operate the manufactured loop type normally, the reservoir under the evaporator needs to be filled with refrigerant, which increases the amount of required refrigerant.

Since heat pipes are installed in high-speed railways and subways, performance measurements were performed under forced convection conditions of 1 m/s to 5 m/s in consideration of the operating environment. The heat load is applied from 1800 W to 4500 W, and

the target performance is less than ΔT 60 K at 2400 W. Both conventional heat type and loop type achieved target performance. Cooling performance ΔT is approximately 5.2% lower in loop type heat pipe than conventional heat pipe on average. Loop type heat pipe has about 8.1% greater cooling capacity and 5.5% lower thermal resistance than conventional heat pipe on average.

In terms of temperature uniformity, the loop type heat pipe was better than conventional heat pipe. In the base test condition, the standard deviation of the loop type was 22% lower than the standard deviation of the conventional type, and the difference between the maximum and minimum temperature was 13% lower. In addition, if the volume of the reservoir for connection is minimized when manufacturing the loop type, the temperature uniformity is expected to be further improved. The temperature uniformity was better in loop type as the heat load increased.

Loop type can be used as a good solution not only for decentralized –power type trains, which are in increasing demand, but also for cooling in a limited space or long–distance heat transport.

References

- [1] Min PyungOh, Lee JungRyul, “Introduction of the next-generation high-speed rail vehicle system (HEMU-430X)” , *The Korean Institute of Electrical Engineers*, Vol.62 No.6 (2013): 30-33.
- [2] Cho HongShik, Park ChoonSoo, “Global high-speed rail technology development trend and domestic technology status” , *The Korean Institute of Electrical Engineers*, Vol.62 No.6 (2013) : 18-23.
- [3] Mun Jinsu, Kim Deokkwang, “Trend and Its Implications of International Railway Market” , *The Korea Transport Institute*, June (2011) : 45-49.
- [4] Chung E.S, Park Y.H, Jang K.H, Kim J.S, Han S.S, “IGBT propulsion system for rolling stock” , *The Korean Society for Railway, Proceeding of the KSR Conference*, (1998) : 226-232.
- [5] Ryoo SeongRyul, Kim SungDae, Ki JaeHyung, Yim KwangBin, Kim ChulJu, “Study on the Design of the Cooling System Used for the Propulsion System of the High-Speed EMU” , *The Korean Society For Railway*, June (2008) : 1208-1213.
- [6] DAEHONG ENTERPRISE Co., LTD, Tech University of Korea, “Heat pipe cooler for next-generation high-speed rail main

- power converter” , *MOTIE*, September (2013) : 21–28.
- [7] Ryoo SeongRyul, Kim SungDae, Ki JaeHyung, Yim KwangBin, Kim ChulJu, “Study on the Design of the Prototype Manufacture of Cooling Systems for the Propulsion System of the EMU” , *The Korean Society For Railway*, November (2008) : 422–429.
- [8] Lee KiWoo, Park KiHo, Lee KyeJung, Ra HoSang, “A Development on Heat Pipe Heat Sink for Cooling the Semiconductor of Subway Train” , *Korea Institute of Energy Research*, August, 1999.
- [9] Cho, TaeSik, “Study on Optical Design of Water Cooling System for Application to Propulsion Systems of HEMU” , 2010, Graduate School of Sungkyunkwan, MD dissertation.
- [10] Xavier Perpiñà, Xavier Jordà, Miquel Vellvehi, Jose Rebollo, Michel Mermet–Guyennet, "Long–term reliability of railway power inverters cooled by heat–pipe–based systems." *IEEE transactions on industrial electronics* 58.7 (2010): 2662–2672.
- [11] Lee JuneSeok, Choi UiMin, "Comparison of heat–pipe cooling system design processes in railway propulsion inverter considering power module reliability." *Energies* 12.24 (2019): 4676.

- [12] David Reay, Peter Kew, Ryan McGlen, “Heat Pipes, Theory, Design and Applications” , sixth edition, BH, (2013) : 149.
- [13] F.J Stenger, “Experimental Feasibility of Water–Filled Capillary–Pumped Heat–Transfer Loops” , *NASA TM X–1310*, NASA, Washington, DC, 1966.
- [14] Y.F.Gerasimov, Y.F. Maydanik, G.T.Shchogolev, et al., “Low–temperature heat pipes with separate channels for vapour and liquid” , *Eng. Phys.J.12(6)*(1975) 957–960 (in Russian).
- [15] Jentung Ku, Laura Ottenstein, Mark Kobel, Paul Rogers, Tarik Kaya, "Temperature oscillations in loop heat pipe operation." *AIP Conference Proceedings*. Vol. 552. No. 1. American Institute of Physics, 2001.
- [16] Zhang Hongxing, Lin Guiping, "Investigation on startup behaviors of a loop heat pipe." *Journal of thermophysics and heat transfer* 19.4 (2005): 509–518.
- [17] Kaya, Tarik, and John Goldak. "Numerical analysis of heat and mass transfer in the capillary structure of a loop heat pipe." *International Journal of Heat and Mass Transfer* 49.17–18 (2006): 3211–3220.
- [18] Storrington, Shane. *Design and manufacturing of loop heat pipes*

- for electronics cooling*. Diss. Carleton University, 2006.
- [19] Ki JaeHyung, Ryo SeongRyoul, Sung ByungHo, Kim, SungDae, Choi Jeehoon, Kim ChulJu, "A Study on Manufacture and Performance Evaluation of a Loop Heat Pipe System with a Cylindrical Evaporator for IGBT Cooling." *Proceedings of the KSR Conference*. The Korean Society for Railway, 2008.
- [20] Lizhan Bai, Guiping Lin, Hongxing Zhang b, Dongsheng Wen, "Mathematical modeling of steady-state operation of a loop heat pipe." *Applied Thermal Engineering* 29.13 (2009): 2643–2654.
- [21] Xianbing Ji, Ye Wang, Jinliang Xu, Yanping Huang, "Experimental study of heat transfer and start-up of loop heat pipe with multiscale porous wicks." *Applied Thermal Engineering* 117 (2017): 782–798.
- [22] Ainur Rosidi, Giarno, Dedy Haryanto, Nursinta Adi Wahanani, Yoyok Dwi Setyo Pambudi, Mukhsinun Hadi Kusuma, "The simulation of heat transfers and flow characterization on wickless loop heat pipe." *Jurnal Polimesin* 20.1 (2022): 29–35.
- [23] Henk Jan van Gerner, "Fluid-selection tool" , *28th European Space Thermal Analysis Workshop*, October 2014.

- [24] Chi, S. W., 'Heat Pipe Theory & Practice,' Hemisphere,
(1976) : 159– 171.
- [25] N. Dunbar, P. Cadell, “Working fluids and Figures of Merit for
CPL/LHP applications” , *CPL-98 Workshop*, (1998).
- [26] Choi JaeBong, “Experimental Study on the Thermal
Performance of a Heat Pipe with Multiple Heat Sources” ,
2021, Graduate School of Korea Aerospace University, MD
dissertation.
- [27] P.D.DUNN, D.A.REAY, “HEAT PIPES” , Fourth Edition,
Pergamon, (1993) : 27–33.
- [28] T.P. Cotter, “Theory of heat pipes” , *LA-3246-MS*, March
1965.
- [29] Chi, S. W., 'Heat Pipe Theory & Practice,' Hemisphere,
(1976) : 79–96
- [30] David Reay, Peter Kew, Ryan McGlen, “Heat Pipes, Theory,
Design and Applications” , sixth edition, BH, (2013) : 30–31.
- [31] B.H.Kim, G.P.Peterson, “Analysis of the critical Weber
number at the onset of liquid entrainment in capillary–driven
heat pipes” , *Int. J. Heat Mass Transfer* 38(8) (1995) 1427–
1442.
- [32] Kim ChulJu, Ko HanSeo, Ryo SeongRyul, Sung ByungHo, Kim

SungDae, Ki JaeHyung, “Design and Analysis of the Cooling System in the Propulsion Control System of the High-Speed EMU” , *Korea Institute of Construction Technology Evaluation*, July (2008) : 29–31.

국 문 초 록

최근 철도 산업은 저탄소, 고효율 운송수단으로 그 중요성이 증대되고 있다. 특히 분산형 동력방식의 고속철도는 집중형 동력방식의 고속철도 대비 가속도와 운송효율이 좋아 관심 받고 있으며, 관련 기술개발도 활발하게 일어나고 있다. 분산형 동력방식의 고속철도는 추진 시스템이 열차마다 각각 설치되어, 냉각을 위한 냉각기 설치 공간에 한계가 있다. 이에 따라 냉각시스템의 냉각성능과 효율적인 공간활용의 중요성이 증대되고 있다.

본 연구에서는 고속철도 및 지하철 추진시스템에 적용되어 있는 반도체 트랜지스터인 IGBT의 냉각을 위하여, 단위 부피당 냉각 열량의 증대와 온도 분포의 균일성을 개선할 수 있는 냉각방법을 연구하였고 루프형 히트파이프를 개선 방안으로 제시하였다.

루프형 히트파이프의 적용 가능성을 분석하기 위해, 지하철에 설치할 수 있는 공간에 설치 가능하며, IGBT의 발열량을 냉각할 수 있는 히트파이프를 설계 및 제작하였다. 루프형 히트파이프의 성능은 별도로 제작한 일반적인 히트파이프와 비교하였다. 루프형 히트파이프의 제작을 위해 이론적 분석이 선행되었으며 정확한 성능을 측정하기 위하여 냉각 시스템의 최적 운전조건에 관한 연구와 실험을 진행하였다. 작동 유체와 충전 비율을 결정하기 위한 실험을 수행하였고, 물을 작동 유체로 34.4%의 충전율로 운전 하였을 경우가 최적 조건임을

실험적으로 확인하였다.

일반적인 히트파이프와 루프형 히트파이프의 실험은 고속철도 또는 지하철 운전 환경을 모사하여 진행하였다. 강제 대류 환경에서 모사한 IGBT의 발열량을 1800 W에서 2400 W까지 상승시켜가며, 각각의 히트파이프의 성능을 비교분석 하였다. 실험결과 루프형 히트파이프를 활용할 경우가 IGBT의 최고온도가 더 낮았으며, 최대 냉각가능 용량도 더 크게 계산되었다. 루프형 히트파이프를 사용하였을 경우와 일반 히트파이프를 사용하였을 경우 모두 IGBT 냉각 성능은 만족하였다. IGBT의 운전 수명을 고려하였을 때, IGBT의 온도 균일성도 중요한 냉각성능이다. 히트 파이프에 의해 냉각된 IGBT의 온도 균일성을 비교하는 실험을 진행하였고, 루프형 히트파이프에서 더 개선된 결과를 얻을 수 있었다.

루프형 히트파이프가 분산형 동력방식에 적용되는 IGBT를 냉각 효율을 증가시킬 수 있음을 실험적으로 증명하였다. 또한 미래 반도체 부품의 고밀도화와 소형화를 고려하였을 때, 루프형 히트파이프는 향후 다양한 방면에 적용 가능한 효율적인 냉각 방법이 될 수 있음을 확인하였다.

주요어 : 루프히트파이프, IGBT모듈, 냉각용량, 온도 균일성, 동력분산형 고속철도

학번 : 2017-26361